General Disclaimer

One or more of the Following Statements may affect this Document

- This document has been reproduced from the best copy furnished by the organizational source. It is being released in the interest of making available as much information as possible.

- This document may contain data, which exceeds the sheet parameters. It was furnished in this condition by the organizational source and is the best copy available.

- This document may contain tone-on-tone or color graphs, charts and/or pictures, which have been reproduced in black and white.

- This document is paginated as submitted by the original source.

- Portions of this document are not fully legible due to the historical nature of some of the material. However, it is the best reproduction available from the original submission.

9950-985

DRL No. 119
DRL Item No. 5
DRD No. SE-5

DOE/JPL-955591-84/11
Distribution Category UC-63

Modelling of Photodegradation in Solar Cell Modules of Substrate and Superstrate Design Made with Ethylene-Vinyl Acetate as Pottant Material

ANNUAL REPORT -- 1983

This work was performed for the Jet Propulsion Laboratory, California Institute of Technology, sponsored by the National Aeronautics and Space Administration under Contract NAS7-100

A. C. Somersall and J. E. Guillet*

University of Toronto

*Principal Investigator

ABSTRACT

A computer model has been developed which can generate realistic concentration versus time profiles of the chemical species formed during photooxidation of hydrocarbon polymers using as input data a set of elementary reactions with corresponding rate constants and initial conditions.

The results of computer simulation have been shown to be consistent with the general experimental observations of the photooxidation of polyethylene exposed to sunlight at ambient temperatures.

The useful lifetime (5% oxidation) of the unstabilized polyethylene is predicted to vary from a few months in hot weather (100°F) to almost two years in cool weather (45°F) with an apparent net activation energy of 10 kcal/mol.

Modelling studies of alternate mechanisms for stabilization of clear, amorphous, linear polyethylene suggest that the optimum stabilizer would be a molecularly dispensed additive in very low concentration which can trap peroxy radicals and also decompose hydroperoxides. In principle, the lifetimes could then be extended over 20 years.

The diffusion of oxygen into the polymer is not rate-limiting to the photooxidation process but edge seals and impervious covers could preclude any autocatalytic photooxidation and thereby extend lifetimes very considerably.

I. INTRODUCTION AND OBJECTIVES

The JPL Flat-Plate Solar Array (FSA) Program has identified a number of possible configurations for modules containing silicon solar cells suitable for construction of solar-energy generating stations and also for small-scale applications involving the use of solar-generated electricity. Although it has been possible to meet many of the original design criteria for the cost of the components of these modules, a most critical feature of the design is that the components should maintain their integrity and function for a minimum efficiency equivalent to 20 years in an outdoor environment which features strong solar UV intensity.

To date, a number of failure and degradation modes have been identified. These include:

1. Soiling
2. Cell cracking/hot spots
3. Interconnect fatigue
4. Structural failure/glass breakage
5. Electrical terminal failure
6. Electrical insulation breakdown
7. Encapsulant thermal degradation
8. ENCAPSULANT PHOTODEGRADATION
9. Delamination
10. Corrosion

Any attempt to develop a technology for producing low-cost, long-life photovoltaic modules and arrays must therefore come to terms with the weathering effects experienced by the materials exposed to the sun's ultraviolet, oxygen, moisture and the stresses imposed by continuous thermal cycling, among other things. Polymeric substances which find application as convenient protective covers, pottants/adhesives and backcovers undergo slow, complex photooxidation which changes the chemical and physical properties of these materials. Absorption of the ultraviolet in the tail of the solar spectrum can cause the breaking of chemical bonds, resulting in embrittlement and increased permeability, or to crosslinking which can produce shrinking and cracks. In addition, oxidation often leads to discoloration and reduced transparency, and to the formation of polar groups which could affect electrical properties.

Much work has already been done to unravel the complexities of the photooxidative processes and to develop some highly effective light (UV) stabilizers which can delay the onset of polymer embrittlement. Excellent reviews have been presented[1]. Some polymer systems have also been exploited to fabricate plastics with controlled lifetimes in the short range [2,3]. However, very little is known about the ultimate changes that occur in polymeric substances after the very long periods of exposure necessary for commercial photovoltaic power plants.

There is no adequate way to predict the rates of the chemical and/or physical changes which occur from accelerated tests. In part, the problem has been that there is no reliable laboratory method to measure these effects inside such extended times. Furthermore, any accelerated tests (in which materials are exposed to higher intensity UV sources in controlled atmospheres) are of limited value in predicting rates since there is usually no reciprocity between intensity and time of exposure.

A new procedure has been adopted in this work directed to developing, for the first time, a reliable predictive capability for the photooxidative lifetime of plastic components, particularly in solar energy modules. The procedure includes the following steps.

1. Identification of failure mechanisms of plastic components of the modules.
2. Determination of the chemical or physical causes of these mechanisms.
3. Development of precise analytical procedures to detect these chemical or physical changes at an early stage.
4. Construction of a computer model using a series of elementary rate equations to describe the chemistry and physics of these changes.
5. Validation of the mathematical model by comparison of data from real but well defined accelerated photochemical systems.
6. Prediction of actual performance lifetime by means of real-time monitoring of early degradation in appropriate outdoor locations and, using the computerized simulation, extrapolation to very much longer times.

Other workers in the FSA project have done ranking studies to select optimal material systems which should have tolerable levels of degradation in 20-25 years and yet meet the other basic design criteria. Of the prime candidates selected as potential pottant materials, an encapsulant grade of a copolymer of ethylene-vinyl acetate (EVA, trade name ELVAX, from DuPont) has emerged as a front-runner beside the alternate poly(n-butyl acrylate) (PnBA). We have, therefore, selected EVA as the polymer for which this new predictive capability will be developed. However, the general method, once refined and demonstrated, should find wide application to a wide variety of synthetic materials where a large number of fundamental reactions gives rise eventually to macroscopic deterioration. Most importantly, this new approach should provide new insight and understanding of this complex photooxidation process which should prove invaluable in the design of new solutions to the problem of stabilization of polymers.

II. THE COMPUTER PROGRAM

Numerical methods for the solution of any large set of coupled differential equations have been developed. The particular method originally due to Gear[4] has been applied by Allara and Edelson for the pyrolysis of alkanes [5] and later by others[6,7] for similar processes. Smog formation and detailed small-molecule photochemistry have also been studied by these numerical simulations[8]. Semi-quantitative prediction has been possible in these cases. However, our work is the first attempt to simulate photooxidation kinetics in the case of polymers.

The computer package necessary to generate concentration-time profiles from a mechanistic model of elementary reactions and rate data was completed in the first two years. Our model now consists of a set of reactions (Table I) for the basic reaction sequence based on the now well established

mechanism of hydrocarbon oxidation. Rate parameters have been assigned to these fundamental equations, based on our best estimates from the literature[9]. The modified program calculates by stepwise integration in real time the varying concentrations of chemical species formed during photooxidation. To validate our numerical procedure we employed the data base given for the cesium flare system and generated curves identical to those of Edelson[10] for the same system. The excellent agreement between predicted and actual rate curves showed that the program itself (irrespective of the data base) is reliable, efficient and versatile and it performs in a satisfactory manner.

III. MECHANISM OF PHOTOOXIDATION

Amorphous Polyethylene

As a starting point for polymer photooxidation we have looked at amorphous high-density polyethylene where we presume that short-range diffusion rates in reaction centres should approach that of viscous liquids. In practice, many polymers will show only chemical changes in the hydrocarbon moiety since bond breakage will commonly take place initially in the more labile C–H and C–C bonds. Initiation will take place following UV absorption by ketone or hydroperoxide groups or even fortuitously by some C–H bond cleavage. The possibilities of energy transfer among different groups have also been included in the model. Propagation takes place via the formation of peroxy radicals followed by hydrogen atom abstraction from the backbone and repeated, fast oxygen-addition. Peroxy radical chain carriers terminate by disproportionation to form alcohols and ketones. Further photolysis of ketone products leads to another autocatalytic chain. The reduced set of important reactions considered and the best literature estimates of corresponding rate constants have been summarized in Scheme I.

Ethylene-Vinyl Acetate Copolymer

Several studies have been carried out on the thermal degradation[11-13], thermal oxidation[14,15] and photooxidation[16] of EVA.

EVA thermally degrades in two stages. Scission of acetoxy groups occurs at 275 to 350°C in a manner similar to that of poly(vinyl acetate) (PVA) causing elimination of acetic acid and giving unsaturation by a molecular chain mechanism involving adjacent acetate units. The hydrocarbon chains of the polymer residue degrade above 400°C. Thus, thermal decomposition of the acetate groups in EVA can be assumed to be negligible at room temperature.

Thermal oxidation of EVA occurs mainly in the PE segments where the usual autocatalytic radical mechanism is analogous to that of polyethylene. The accompanying thermal degradation of the vinyl acetate units results in the evolution of acetic acid and generation of unsaturation, as mentioned previously. Subsequent oxidation of the unsaturation was reported to produce various carbonyl-containing compounds, including aldehydes, ketones

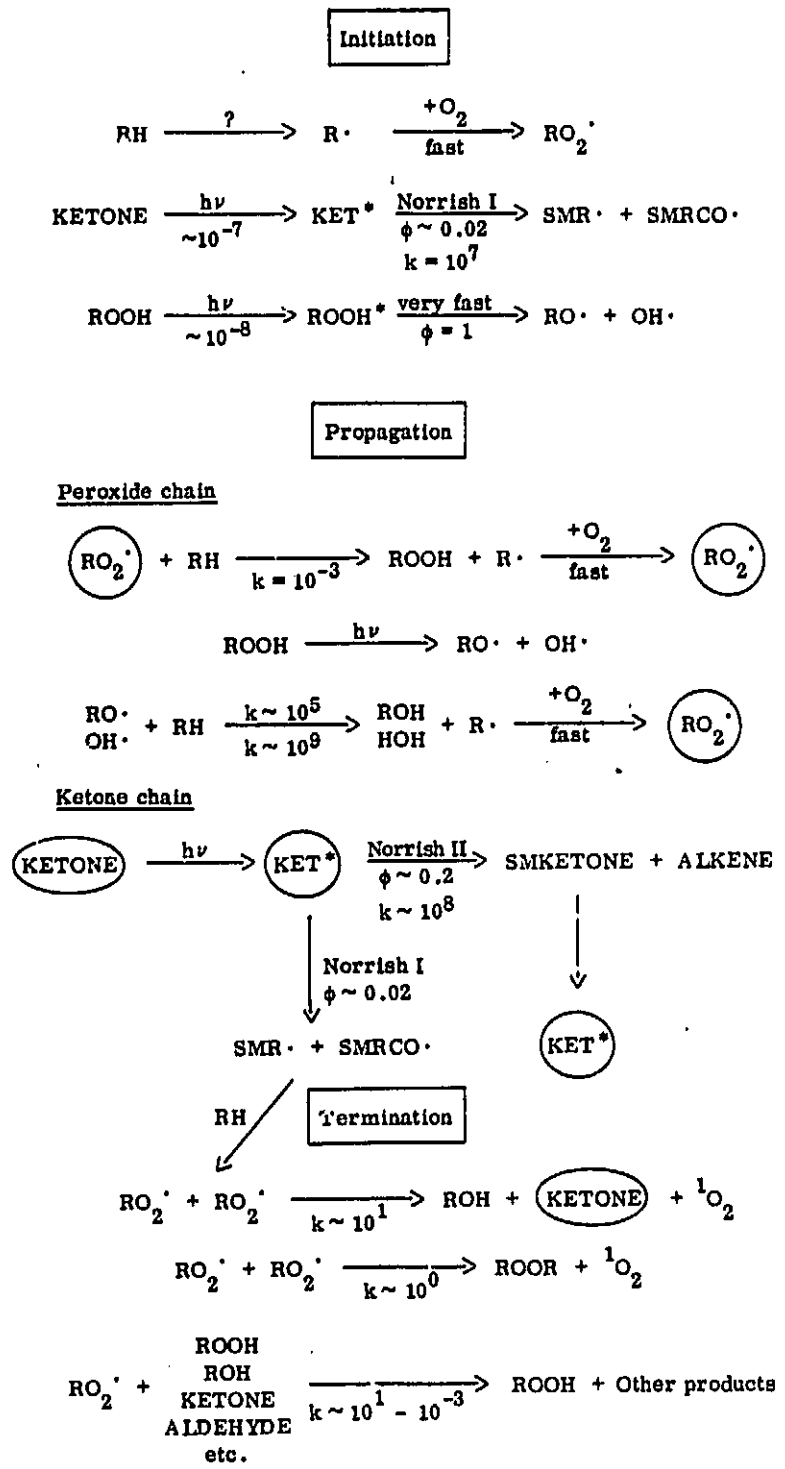

SCHEME . Polyethylene photooxidation scheme.

esters and acids. Again, it is apparent that thermal oxidation will be limited to the PE moiety at ambient temperatures.

The photooxidation of EVA has been reported only by Lugova et al. [16] employing UV irradiation in air at room temperature. Their work suggests that the oxidation of the ethylene units and the photoreactions of the acetate chromophores proceed independently of each other, essentially in a parallel fashion.

The above results indicate that a generalized mechanism of photooxidation of EVA can be constructed using the known polyethylene photooxidation mechanism as a model for reactions expected to occur in the hydrocarbon portion of EVA. Similarly, information can be extracted from studies of the photooxidation of PVA and of acrylate polymers which allows formulation of the fundamental photochemical processes expected for the acetate groups in EVA. Some modifications to the present model for polyethylene will therefore be necessary to allow for the differences due to substitution in EVA.

IV. COMPUTER MODELLING OF PHOTOOXIDATION

We have already shown that many of the general experimental observations in the photooxidation of hydrocarbon polymers can be accounted for by computer simulation, using the elementary mechanism and corresponding rates (e.g., Figure 1). Computer simulations of photooxidation for amorphous linear hydrocarbons have shown the following patterns of general behavior.

1. The time to failure, τ_f (chosen as the level of 5% C–H bond oxidation, which is within the range we would anticipate for marked change in mechanical properties) varies as the inverse square root of the light intensity (Figure 2). However, τ_f is almost unaffected by both the photoinitiator type and concentration (Figure 3).
2. The time to failure decreases with the rate of abstraction of C–H by peroxy radicals (Figure 4) but increases with the rate of bimolecular radical termination controlled by diffusion (Figure 5).
3. Of the various stabilization mechanisms considered (Scheme II), the trapping of peroxy radicals is distinctly the most effective (Figure 6), although the concommitant decomposition of hydroperoxide is also desirable (Figure 7).
4. For a partially crosslinked polymer where the physical properties are not steep functions of crosslink density, it is unlikely that there will be dramatic failure modes due to net changes in molecular weight of the polymers (Figures 8-10).
5. Energy loss (power loss) due to polymer light absorption (with yellowing discoloration) will not be a significant failure mode (Figure 11).

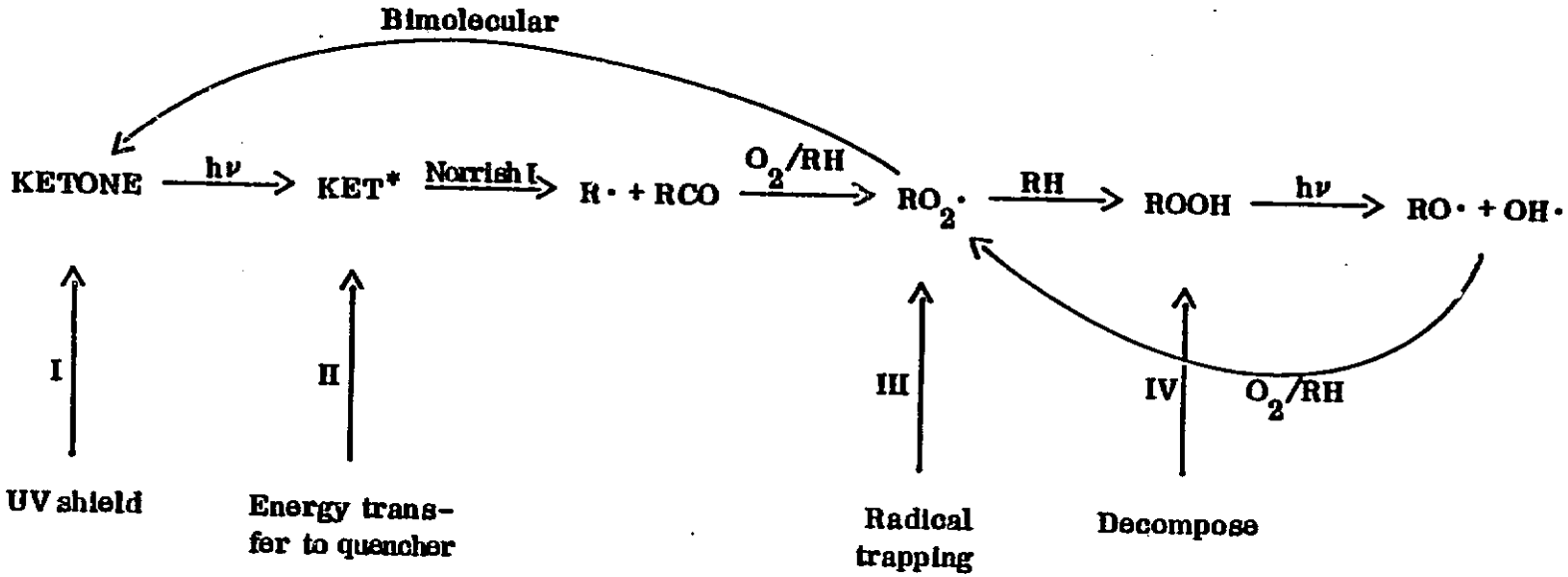

Scheme II. Stabilisation mechanisms

6. Since the all-important peroxy radicals terminate by bimolecular disproportionation, at low concentrations they could have lifetimes of up to several hours, which would affect the extent of dark reactions in the daily cycle during outdoor applications (Figure 12).

V. THE EFFECT OF TEMPERATURE

For outdoor applications, the variation of temperature will have important effects on the useful lifetimes of hydrocarbon polymers. This has been the focus of the past year. To accommodate thermal variables, the rate constants were expressed in terms of the Arrhenius parameters, A (the pre-exponential factor) and E (the activation energy). This naturally multiplied the mathematical complexity in the program which now has more than 100 different parameters. Many of the species in the complex process undergo a number of competitive pathways, the relative importance of each being often sensitive to small changes in the calculated rate constant values. In addition, the different magnitudes of the activation energy caused various changes in the relative importance of the different key processes of propagation and termination with changes in operating temperature. No attempt has been made as yet to model thermal oxidation at elevated temperature, but even at moderate outdoor temperature (100°F) the decomposition of hydroperoxides does become significant.

$$ROOH \xrightarrow{\Delta} RO^{\cdot} + OH^{\cdot}$$

Five such decomposition reactions (numbers 52 to 56) were then included in the basis set (Table I).

Figure 13 shows the variation of time to failure (5% oxidation) with temperature. The decrease in lifetime with no stabilizer is more or less as expected, ranging from a few months in hot tropical weather, 310 K (100°F), to almost two years in cool weather, 280 K (45°F). An attempt at a typical Arrhenius plot (Figure 14) shows an "apparent net activation energy" of 10-16 kcal/mol near atmospheric temperatures (280-310 K). Experimental values of 16-35 kcal/mol for the dependence of the induction period in polyethylene oxidation have been reported at temperatures above 380 K [17]. For thick films the observed value is as low as 10 kcal/mol [18].

VI. OXYGEN-DIFFUSION

We have re-examined more closely the importance of oxygen addition to carbon-centred radicals in our mechanistic scheme. Until now, we had assumed that in air, there is a sufficient concentration of oxygen dissolved in the polymer (10^{-3} M) and the rate of addition to carbon-centred radicals was so fast $k > 10^9$) that all other reactions of the latter were excluded. In fact, the products of those reactions leading to carbon-centred radicals were written as peroxy radicals in one concerted step.

In the gas phase, the rate of oxygen addition to ethyl radicals has been measured at 4.2×10^9 by Sleepy and Calvert [19]. In solution, there are no data for reaction of alkyl radicals with oxygen because the reaction is so fast that the oxygen pressure must be maintained at a very low value [20]. But in the polymer phase, the question remains whether the addition is truly limited by diffusion or alternatively the static model of Perrin [21] is more appropriate -- namely, that each carbon-radical centre will inevitably add any oxygen molecule found within a finite sphere so that the rate shows a dependence only on the distribution related to concentration.

To examine this we replace all the alkyl radical-producing equations,

$$X \longrightarrow RO_2^{\cdot} \quad \text{or} \quad SMRO_2^{\cdot}$$

with two independent steps, (i) followed by (ii):

$$X \xrightarrow{(i)} R^{\cdot} \xrightarrow[O_2]{(ii)} RO_2^{\cdot}$$

$$X' \longrightarrow SMR^{\cdot} \longrightarrow SMRO_2^{\cdot}$$

In addition, we also included other reactions of alkyl radicals such as recombination, disproportionation, H-abstraction and addition to other radical intermediate species. We could then vary the rate of oxygen addition (related to diffusion).

$$-(d/dt)[R^{\cdot}] = k_{54}[R^{\cdot}][O_2]$$

Under typical conditions, the concentration of alkyl radicals ($R^{\cdot}$) was of the order of 10^{-16} M which is exceedingly low. We found that for autoacceleration to occur the rate constant $k_{54} \sim 10^{-15}$ which is obviously too fast for any dynamic (collisional) process, suggesting that the static quenching model may be more appropriate (with a quenching sphere of radius $\sim$70 Å, corresponding to a distribution of 10^{-3} M oxygen).

Alternatively, autoacceleration does occur if the concentration of alkyl radicals is increased by making the light intensity levels two to four orders of magnitude greater. This would be arbitrary, though, having no experimental basis in outdoor application. Thus, even in the induction period, the autocatalysis by the peroxy radicals is necessary to generate the levels of radical concentration to observe photooxidation in any reasonable time frame. It is also this early influence of the peroxy radicals which makes the process almost insensitive to the nature and concentration of initiator.

It seems therefore that, in practice, the diffusion of oxygen is not rate limiting to the photooxidation process in air. The rate of photooxidation is too slow without autocatalysis and the autocatalysis becomes independent of the diffusion rate as long as this rate can replenish the oxygen consumed to maintain its steady concentration, typically of order 10^{-3} M.

In some practical designs, it may be convenient to use edge seals and impervious covers such as glass which could preclude any autocatalytic photooxidation and thereby extend lifetimes very considerably.

VII. ACCELEROMETER STUDIES

In support of the computer modelling of the photodegradation of polymers being carried out at the University of Toronto, EcoPlastics Limited have studied the effect of exposure of several polymer systems to photooxidation in a UV Accelerometer. The intent was to use samples of ethylene/vinyl acetate (EVA) copolymers provided by Springborn Laboratories. However, the samples were not in a suitable form for either accelerated weathering or outdoor exposure. It is understood that samples of the polymers to be used in practical FSA applications are crosslinked and do not show the problems evidenced by the samples received. The latter showed problems of flow and sag at temperatures greater than 35°C and excessive tackiness which resulted in significant buildup of dirt on the samples, expecially those exposed outdoors.

In the tests reported here, therefore, polyethylene copolymers containing various types of carbonyl groups were exposed to accelerated weathering and the photooxidation was monitored by the buildup of carbonyl functions as determined by the infrared spectra.

Apparatus Used

The American Ultraviolet Co. UV Accelerometer consists of a medium pressure lamp in the centre of a cylinder. The samples were placed on the cylinder which was then rotated around the lamp. The lamp is enclosed by a Pyrex tube which effectively screens out any unwanted low wavelength light. The major components of the lamp are of 298 and 313 nm wavelength. The lamp generates some heat and the samples were subjected to temperatures of 38-42°C during exposure.

The carbonyl absorbance of the compression-molded films was measured on a Bausch and Lomb Spectronic 250 IR over the range 2000 - 1250 cm^{-1}. In order to minimize the effects of variation of absorbance at 1710 cm^{-1} with thickness, the absorbance is normalized by dividing out the absorbance of a CH-bending motion transition of the polymer observed at 1375 cm^{-1}. Thus the results are presented as

$$Z = A_{1710}/A_{1375}$$

where A_{1710} is the absorbance of the film at 1710 cm^{-1} and A_{1375} is the absorbance of the film at 1375 cm^{-1}.

The hours of exposure in the Accelerometer were converted into incident dose by means of an actinometer which monitors the photodegradation of a polystyrene/methyl isopropenyl ketone copolymer by determining its

decrease in molecular weight on irradiation. The polymeric actinometer has been calibrated against a chemical actinometer from which the incident dose on the samples in Joule/cm^2 at 313 nm can be calculated. Thus the results to be reported here give the amount of carbonyl functions Z as a function of the incident dose.

Irradiation was continued until the film became brittle. Brittleness was measured by the ability of the film to withstand creasing. The film was bent back on itself and a crease formed by applying finger pressure on the bend. If the film broke at the crease, or broke as it was returned to its flat position, it was considered brittle.

Materials

The following polymers were tested.

1. Low density polyethylene (Union Carbide).
2. Ethylene/carbon monoxide copolymer containing 1% w/w carbon monoxide (Eastman Kodak).
3. Ethylene/methyl isopropenyl ketone copolymer containing 2% w/w methyl isopropenyl ketone (Dutch State Mines).
4. Ethylene/carbon monoxide copolymer containing 3% w/w carbon monoxide Eastman Kodak).
5. A graft terpolymer of ethylene, methyl vinyl ketone and styrene containing 3% methyl vinyl ketone and 3% styrene.
6. A blend of low density polyethylene (polymer no. 1) and an ethylene/carbon monoxide copolymer (polymer no. 2) in the ratio 80 parts polymer no. 1 to 20 parts polymer no. 2.
7. A blend of low density polyethylene (polymer no. 1) and an ethylene/methyl isopropenyl ketone copolymer (polymer no. 3) in the ratio 80 parts polymer no. 1 to 20 parts polymer no. 3.

The blends were prepared on a two-roll mill and other samples were worked on the mill for the same length of time (3 min) to ensure similar thermal history before irradiation. Films were prepared by compression molding in a Carver press using 20,000 psi for 30 s at 180°C. Samples were cut to be 4 cm x 1 cm x 80 ± 5 μm. The samples were then attached to a holder.

Weathering

The samples were exposed to the UV light of the Accelerometer for set periods of time and then removed for testing. Initially only the infrared spectrum was measured but as degradation proceeded, the films were also tested for brittleness. Two samples of each composition were exposed, only one of which was tested for brittleness since too many creases would affect the results. When the creased film became brittle, the result was confirmed by testing the second film. If this film was not brittle, exposure was continued until brittleness was achieved. Unless the required exposure

was more than a further exposure period, the difference is not noted. The results are given in Table 2 and shown graphically in Figure 15.

It will be observed that while most of the films become brittle at a Z value of 6 or higher, sample no. 3, the MIPK/ethylene copolymer, becomes brittle at a Z value of about 4. This is not surprising since this polymer has a high efficiency of chain scission which does not necessarily lead to formation of oxygenated species.

The general observation that the absorbance shows a linear dependence on the dose of incident UV is consistent with the predictions of the computer model[22]. The apparent induction period shown for low-density polyethylene and the blend of polyethylene and a copolymer with carbon monoxide underlines the importance of modelling the chemical changes taking place long before the physical effects become apparent.

REFERENCES

1. (a) D. J. Carlsson, A. Garton and D. M. Wiles, Developments in Polymer Statilisation -- 1, G. Scott, Ed., Applied Science, Barking, 1980; (b) V. Ya. Shlyapintokh, Developments in Polymer Photochemistry -- 2, N. S. Allen, Ed., Applied Science, Barking, 1980, p.215; (c) W. B. Hardy, Developments in Polymer Photochemistry -- 3, N. S. Allen, Ed., Applied Science, Barking, 1980, p.287.

2. J. E. Guillet, Polymers and Ecological Problems, J. E. Guillet, Ed., Plenum Press, New York, 1973.

3. G. Scott, J. Polym. Sci., Polym. Symposia, 57, 357 (1976).

4. C. W. Gear, Commun. ACM, 14, 176 (1971).

5. D. L. Allara and D. Edelson, Int. J. Chem. Kinet., 7, 479 (1975).

6. K. M. Sundaram and G. F. Froment, Ind. Eng. Chem. Fundamen., 17(3), 174 (1978).

7. D. B. Olson, T. Tanzawa and W. C. Gardiner, Jr., Int. J. Chem. Kinet., 11, 23 (1979).

8. (a) K. H. Ebert, H. J. Ederer and G. Isbarn, Angew. Chem., 19, 333 (1980); (b) L. Farrow and D. Edelson, Int. J. Chem. Kinet., 6, 787 (1974); (c) W. P. L. Carter, A. C. Lloyd, J. L. Spring and J. N. Pitts, Jr., ibid., 11, 45 (1979); (d) R. Hiatt, U. G. K. Nair, Can. J. Chem., 57, 450 (1979).

9. We acknowledge useful consultations on this subject with Dr. Keith Ingold of the National Research Council of Canada, and Dr. J. R. MacCallum of the University of St. Andrews. Any omissions or errors are ours.

10. D. Edelson, J. Chem. Ed., 52, 642 (1975).

11. I. C. McNeill, A. Jamieson, D. J. Tosh and J. J. McClure, Eur. Polym. J., 12, 305 (1976).

12. D. L. Gardner and I. C. McNeill, J. Thermal Analysis, 1, 389 (1969).

13. D. Munteanu and S. Turcu, Chem. Abstr. 80:198053y, 80:44478d (1973).

14. L. I. Lugova, V. M. Demidova and F. O. Pozdnyakova, Chem. Abstr. 81:153092p (1974).

15. J. Kajaks, V. Kranbergs, A. B. Vainshtein and V. Kardivans, Chem. Abstr. 84:75621z (1978).

16. L. I. Lugova, F. O. Pozduyakova, G. S. Popova and A. F. Lerkovnikov, Chem. Abstr. 85:124583s (1976).

17. (a) J. E. Wilson, Ind. Eng. Chem., 47, 2201 (1955); (b) G. W. Blum, J. R. Shelton, and H. Winn, ibid., 43, 464 (1951).

18. H. H. G. Jellinek, S. N. Lipovac, Macromolecules, 3, 231, 237 (1970).

19. W. C. Sleepy and J. C. Calvert, J. Am. Chem. Soc., 81, 769 (1959).

20. T. Mill and D. G. Hendry, Comp. Chem. Kinet., 16, 27 (1980).

21. F. Perrin, C. R. Acad. Sci. Paris, 178, 1978 (1924).

22. J. E. Guillet, Pure Appl. Chem., 52, 285 (1980).

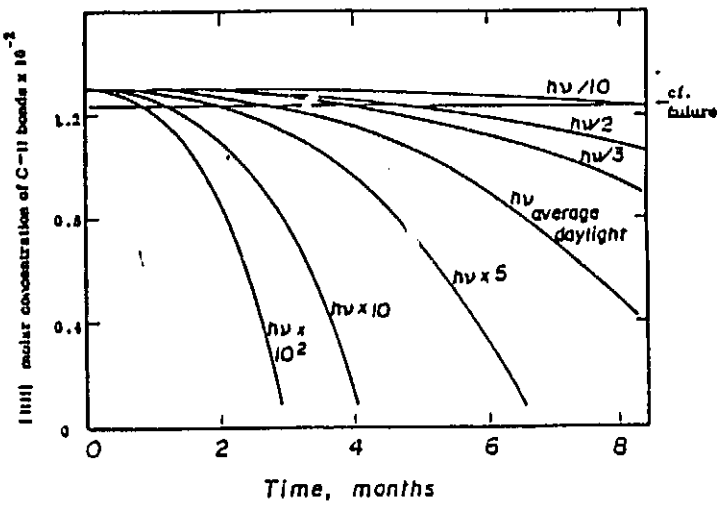

FIGURE 1. Photooxidation of unstabilized PE.

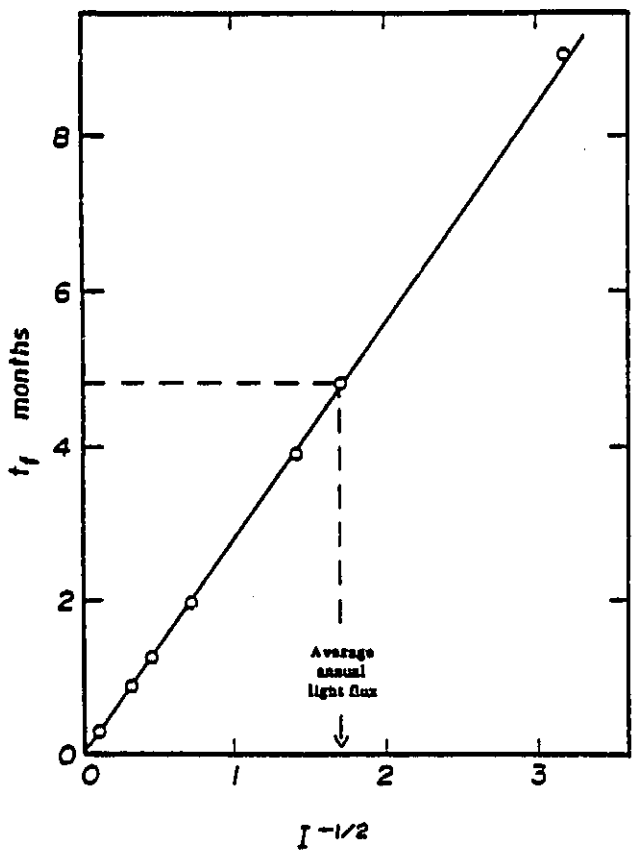

FIGURE 2. Photooxidation of unstabilized PE. Time to failure as a function of light intensity.

$$\text{ROOH} \xrightarrow{h\nu} \text{RO}\cdot + \text{OH}\cdot$$

$$\text{Ketone} \xrightarrow{h\nu} \text{R}\cdot + \text{R}\dot{\text{C}}{=}\text{O}$$

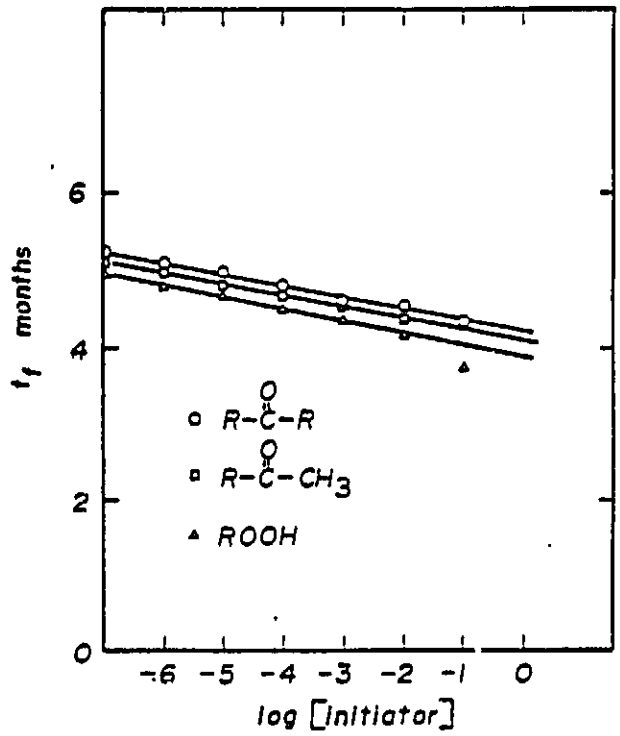

FIGURE 3. Photooxidation of unstabilized PE. Time to failure as a function of initiator type and concentration.

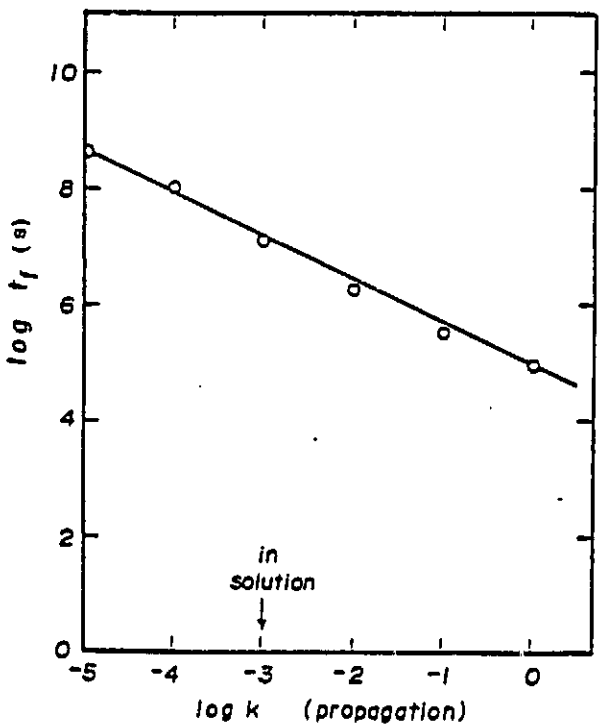

FIGURE 4. Photooxidation of unstabilized PE. Time to failure as a function of propagation rate constant.

$$RO_2\cdot + RH \xrightarrow{k_p} ROOH + R\cdot \xrightarrow{O_2} RO_2\cdot$$

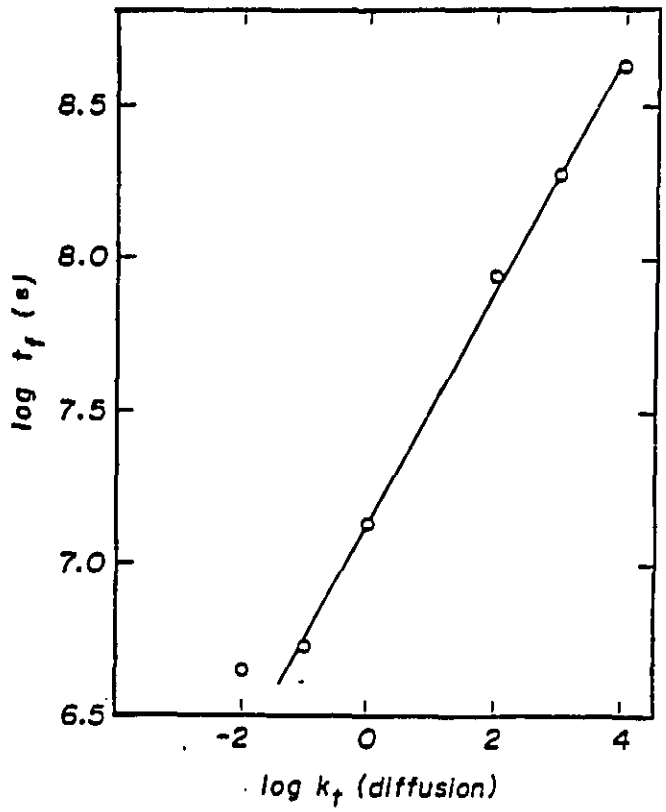

FIGURE 5. Photooxidation of unstabilized PE. Effect of bi(macro)molecular diffusion (radical termination on time to failure, e.g.,

$$RO_2\cdot + RO_2\cdot \xrightarrow{k_t} \text{Products}$$

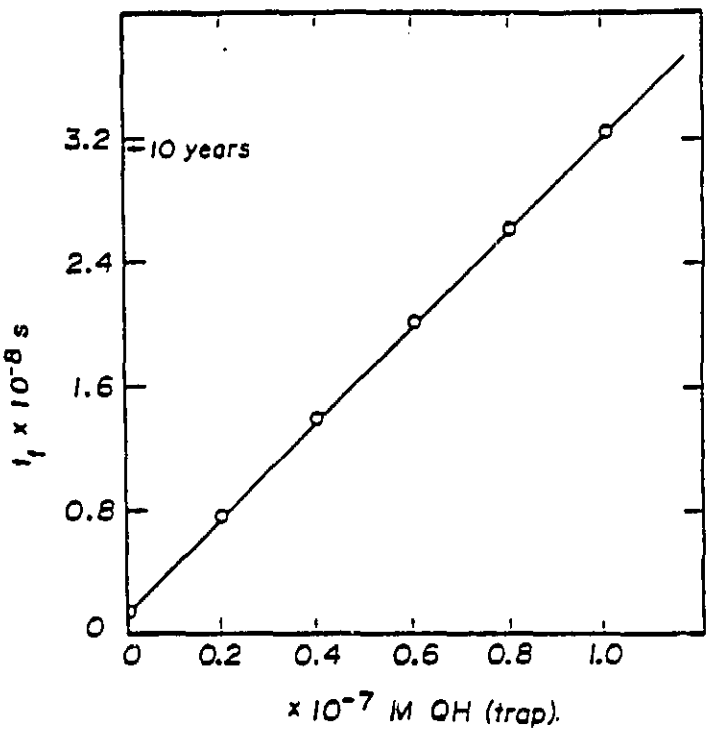

FIGURE 6. Stabilization of PE by radical trapping (very low molecular concentration).

$$RO_2\cdot + QH \xrightarrow{10^6} ROOH + Q$$

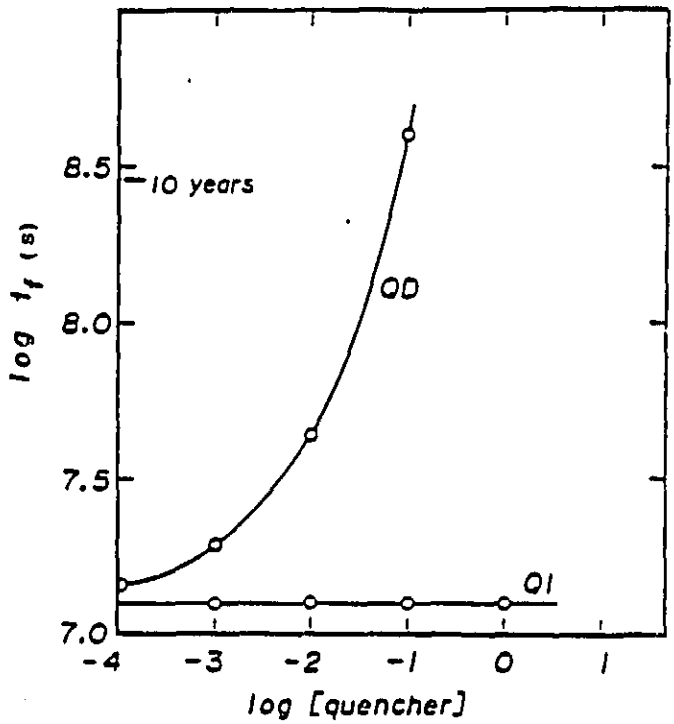

FIGURE 7. Stabilization of PE.

$$ROOH + QD \xrightarrow{10^6} \text{Products}$$

$$KET^* + Q_1 \xrightarrow{10^6} \text{Ketone} + \text{Heat}$$

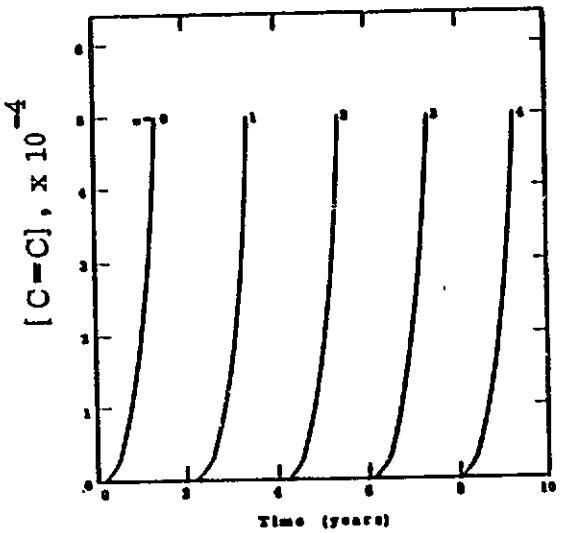

FIGURE 8. Effect of stabilizer on alkene formation. Stabilizer concentration, c (x 10^{-6} wt-%).

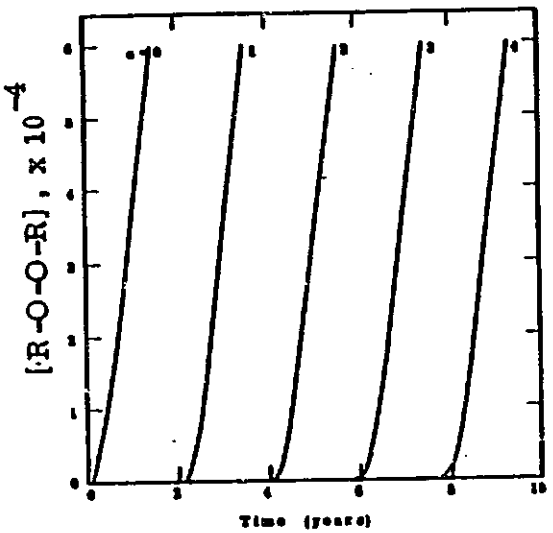

FIGURE 9. Effect of stabilizer on formation of crosslinks. Stabilizer concentration, c (x 10^{-6} wt-%).

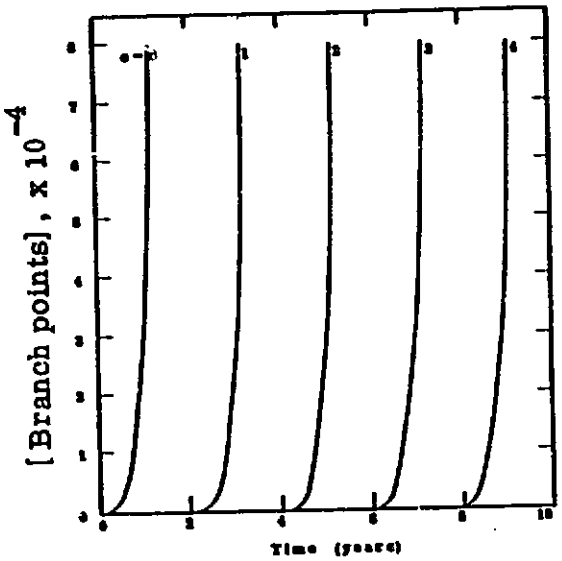

FIGURE 10. Effect of molecularly dispersed stabilization on formation of branch points. Stabilizer concentration, c (x 10^{-6} wt-%).

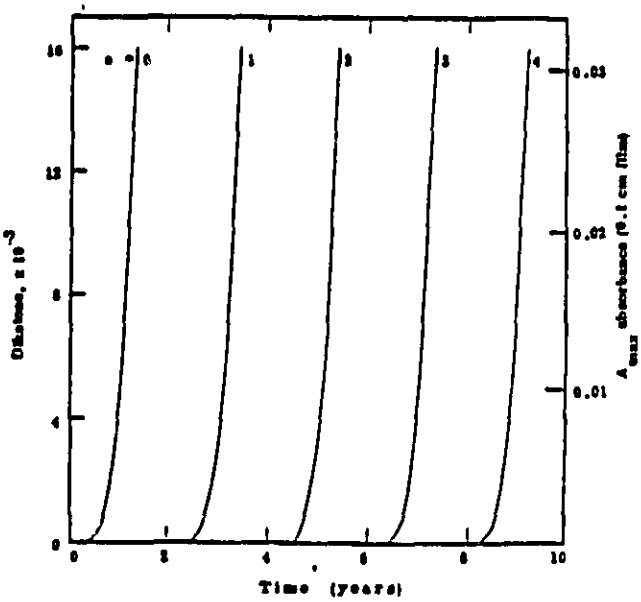

FIGURE 11. Effect of molecularly dispersed stabilizer on diketone formation. Stabilizer concentration, c (x 10^{-6} wt %).

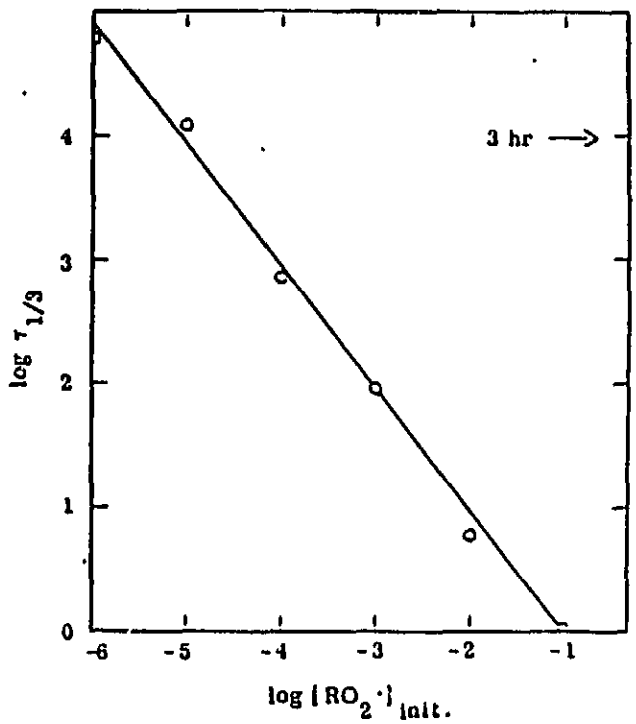

FIGURE 12. Lifetime of peroxy radicals in the dark. ($\tau_{1/3}$ in sec)

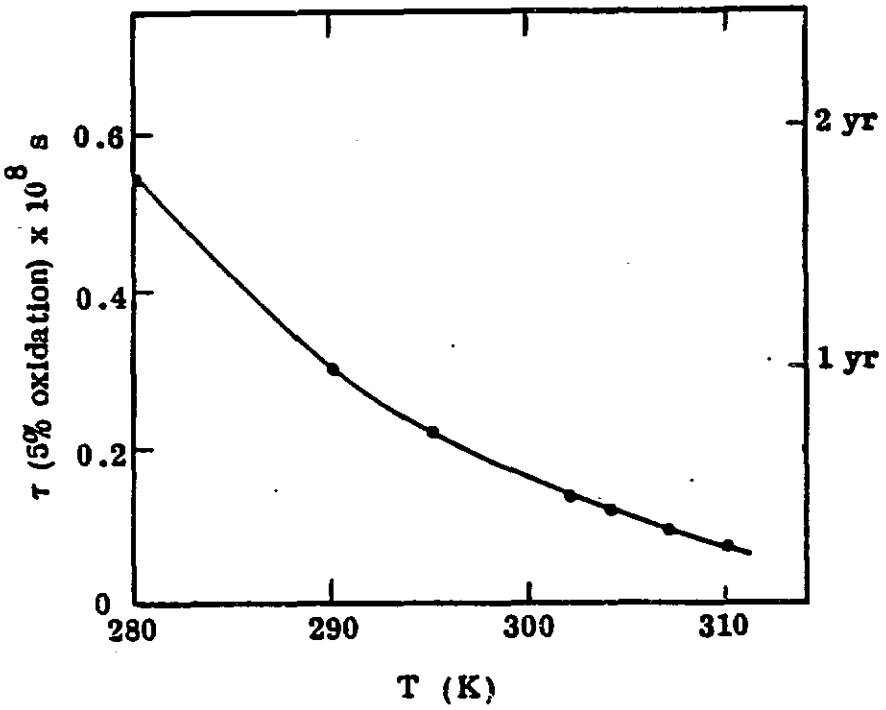

FIGURE 13. Time to failure (5% oxidation) as a function of temperature.

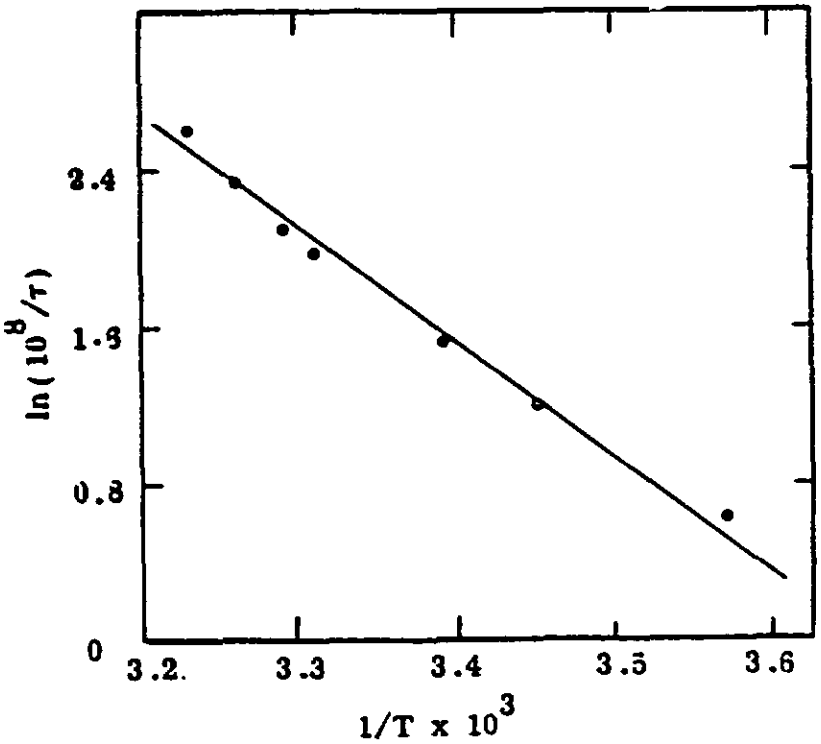

FIGURE 14. Arrhenius plot of the rate of oxidation (k vs. 1/T).

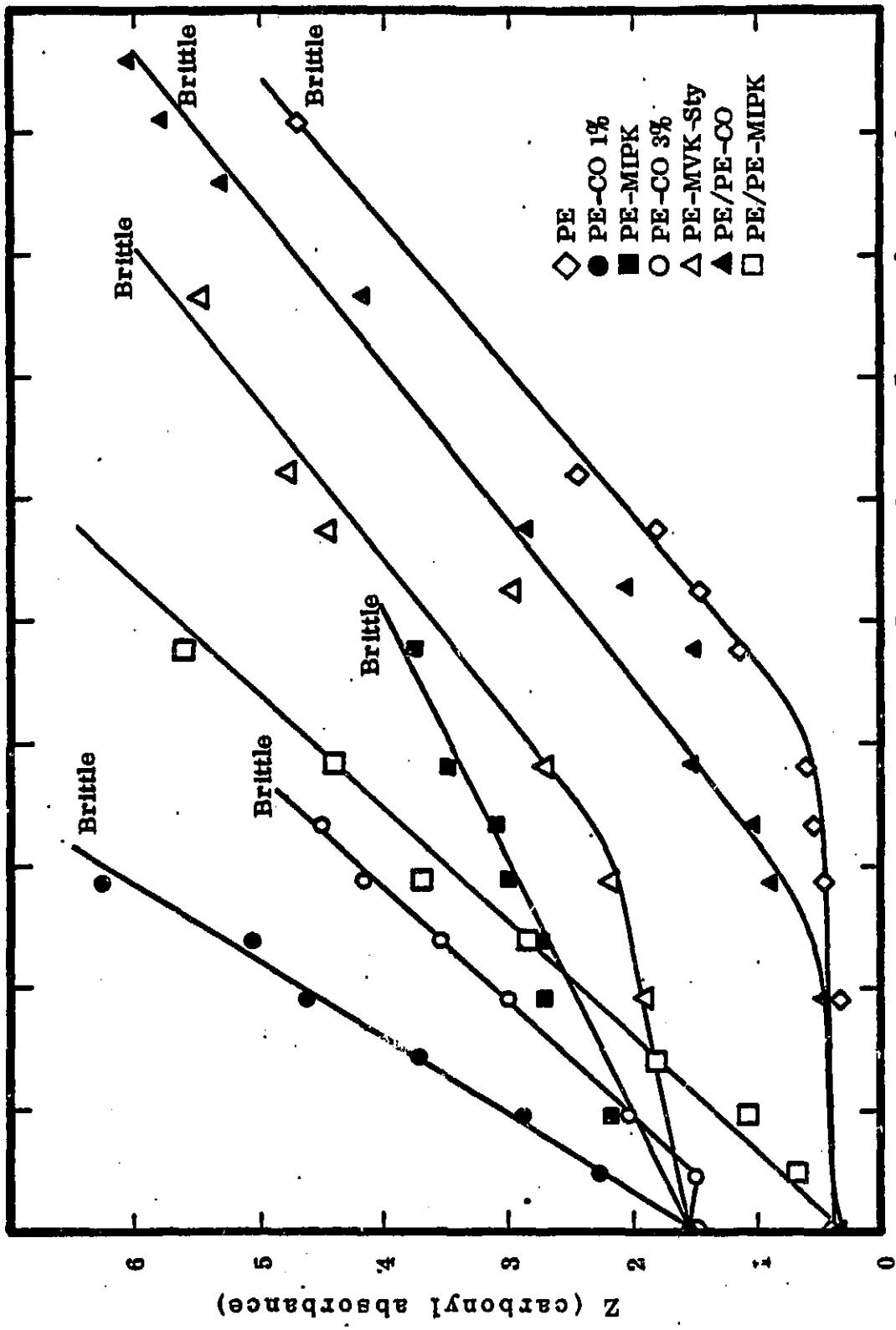

FIGURE 15. Photooxidation of carbonyl-containing polymers.

TABLE 1. Data Set: Photooxidation Reaction Scheme and Activation Parameters

	Reaction matrix		A	E kcal/mol
1.	Ketone	$\longrightarrow$ KET*	0.70×10^{-9}	0
2.	KET*	$\longrightarrow$ $SMRO_2$ + SMRCO	0.59×10^{9}	4.8
3.	SMRCO	$\longrightarrow$ $SMRO_2$ + CO	0.80×10^{17}	15
4.	KET*	$\longrightarrow$ Alkene + SMKetone	0.56×10^{8}	2.0
5.	SMKetone	$\longrightarrow$ SMKET*	0.70×10^{-9}	0
6.	SMKET*	$\longrightarrow$ $SMRO_2$ + CH_3CO	0.32×10^{13}	8.5
7.	SMKET*	$\longrightarrow$ Alkene + Acetone	0.56×10^{9}	2.0
8.	RCOH	$\longrightarrow$ RO + OH	0.13×10^{9}	0
9.	RO_2 + RH	$\longrightarrow$ ROOH + RO_2	0.10×10^{10}	17.0
10.	$SMRO_2$ + RH	$\longrightarrow$ SMROOH + RO_2	0.10×10^{10}	17.0
11.	SMROOH	$\longrightarrow$ SMRO + OH	0.13×10^{-9}	0
12	SMRO + RH	$\longrightarrow$ SMROH + RO_2	0.16×10^{10}	6.2
13.	RO + RH	$\longrightarrow$ ROH + RO_2	0.16×10^{10}	6.2
14.	RO	$\longrightarrow$ $SMRO_2$ + Aldehyde	0.32×10^{16}	17.4
15.	KET* + ROOH	$\longrightarrow$ Ketone + RO + OH	0.25×10^{10}	11.6
16.	SMKET* + RCOH	$\longrightarrow$ SMKetone + RO + OH	0.25×10^{10}	11.6
17.	SMRCO + O_2	$\longrightarrow$ SMRCOOO	0.80×10^{14}	9.6
18.	SMRCO + RH	$\longrightarrow$ RO_2 + Aldehyde	0.10×10^{10}	7.3
19.	SMRCOOO + RH	$\longrightarrow$ SMRCOOOH + RO_2	0.10×10^{10}	17.0
20.	SMRCOOOH	$\longrightarrow$ SMRCOO + OH	0.13×10^{-9}	0
21.	SMRCOO	$\longrightarrow$ $SMRO_2$ + CO_2	0.10×10^{15}	6.6
22.	SMRCOO + RH	$\longrightarrow$ Acid + RO_2	0.10×10^{10}	17.0
23.	OH + RH	$\longrightarrow$ RO_2 + Water	0.10×10^{10}	.0.5
24.	CH_3CO + RH	$\longrightarrow$ RO_2 + CH_3CHO	0.10×10^{10}	7.3
25.	CH_3CO + O_2	$\longrightarrow$ CH_3COOO	0.89×10^{14}	9.6
26.	CH_3COOO + RH	$\longrightarrow$ CH_3COOOH + RO_2	0.10×10^{10}	17.0
27.	CH_3COOOH	$\longrightarrow$ CH_3COO + OH	0.13×10^{-9}	0
28.	CH_3COO + RH	$\longrightarrow$ CH_3COOH + RO_2	0.10×10^{15}	6.6
29.	KET*	$\longrightarrow$ Ketone	0.10×10^{9}	0
30.	SMKET*	$\longrightarrow$ SMKetone	0.10×10^{9}	0
31.	KET* + O_2	$\longrightarrow$ Ketone + SO_2	0.89×10^{14}	9.6
32.	SMKET* + O_2	$\longrightarrow$ SMKetone + SO_2	0.89×10^{14}	9.6
33.	RO_2 + RO_2	$\longrightarrow$ ROH + Ketone + SO_2	0.25×10^{10}	11.6
34.	RO_2 + ROH	$\longrightarrow$ ROOH + Ketone + HOO	0.10×10^{10}	15.3
35.	HOO + RH	$\longrightarrow$ HOOH + RO_2	0.32×10^{9}	15.0
36.	HOO + RO_2	$\longrightarrow$ ROOH + SO_2	0.32×10^{9}	2.1
37.	RO_2 + Ketone	$\longrightarrow$ ROOH + PeroxyCO	0.13×10^{5}	8.9
38.	PeroxyCO + RH	$\longrightarrow$ PEROOH + RO_2	0.10×10^{10}	17.0
39.	PERCOH	$\longrightarrow$ PERO + OH	0.13×10^{-9}	0
40.	PERO + RO_2	$\longrightarrow$ DIKetone + ROOH	0.25×10^{10}	11.6
41.	RO_2 + ROOH	$\longrightarrow$ ROOH + Ketone + OH	0.25×10^{8}	11.6
42.	RO_2 + SMROH	$\longrightarrow$ ROOH + Aldehyde + HOO	0.10×10^{10}	15.3
43.	RO_2 + Aldehyde	$\longrightarrow$ ROOH + SMRCO	0.25×10^{10}	11.6
44.	RO_2 + RO_2	$\longrightarrow$ ROOR + SO_2	0.38×10^{12}	16.0
45.	SO_2	$\longrightarrow$ O_2	0.63×10^{5}	0
46.	SO_2 + Alkene	$\longrightarrow$ ROOH	0.20×10^{14}	10.0
47.	RO_2 + Alkene	$\longrightarrow$ Branch	0.16×10^{9}	11.6
48.	$SMRO_2$ + Alkene	$\longrightarrow$ ROOH	0.16×10^{9}	11.6
49.	RO_2 + QH	$\longrightarrow$ ROOH + Q	0.16×10^{8}	5.2
50.	KET* + Q1	$\longrightarrow$ Ketone + Heat	0.80×10^{13}	9.5
51.	ROOH + QD	$\longrightarrow$ PRODS	0.80×10^{13}	9.5
52.	ROOH	$\longrightarrow$ RO· + OH·	0.63×10^{15}	35
53.	SMROOH	$\longrightarrow$ SMRO + OH	0.63×10^{15}	35
54.	SMRCOOOH	$\longrightarrow$ SMRCOO + OH	0.63×10^{15}	35
55.	CH_3COOOH	$\longrightarrow$ CH_3COO + OH	0.63×10^{15}	35
56.	PEROOH	$\longrightarrow$ PERO + OH	0.63×10^{15}	35

TABLE 2. Photooxidation of Carbonyl-Containing Polymers

Incident dose, kJ	Sample Z (carbonyl absorbance)[a]									
	1	2	2	3	3	4	5	6	7	7
0	0.41	1.50	1.50	1.55	1.55	1.60	1.58	0.38	0.41	0.37
0.48			2.27		1.50					0.63
0.96			2.89	2.18	2.04					1.07
1.43			3.73			2.15	1.84			
1.91	0.33		4.62		3.01	2.96	1.91	0.48	1.79	2.72
2.39		4.16	5.06	2.86	3.55	3.57				2.76
2.87	0.46	7.31	6.27	2.98	4.14	3.58	2.18	0.89	3.00	3.67
3.35	0.55	Brittle[b]	Brittle	3.10	4.50	4.28		1.04	3.62	5.06
3.82	0.61			3.50	Brittle	5.33	2.71	1.52	4.09	4.39
4.78	1.15			3.74		Brittle		1.52	4.98	5.60
5.26	1.47			Brittle			2.97	2.07	4.73	7.19
5.74	1.82						4.47	2.86	6.39	Brittle
6.21	2.43						4.76		Brittle	
7.65							5.47	4.17		
8.60								5.23		
9.08	4.67						5.77	5.77		
9.56							6.32	6.05		
11.47							Brittle	Brittle		
12.43	7.92									
12.91	10.00 Brittle									

[a] Samples of same number are duplicate runs of same material.

[b] Brittle at time of last value of Z recorded.

Ecoplastics

OUTDOOR WEATHERING
and
ACCELERATED AGEING TESTS
on
ETHYLENE-VINYL ACETATE COPOLYMERS

FINAL REPORT 1983

Prepared by: EcoPlastics Limited,
518 Gordon Baker Road,
Willowdale, Ontario,
M2H 3B4.

Prepared for: Professor J. E. Guillet,
University of Toronto,
Department of Chemistry,
80 St. George Street,
Toronto, Ontario,
M S 1A1.

I. Summary

Experimental measurements have been made of the changes in the ultraviolet and infrared absorbance spectra of various polymer films exposed to solar and simulated solar radiation. Polymers tested include polyethylene (PE), ethylene vinyl acetate copolymer (EVA) and a stabilized ethylene vinyl acetate copolymer (A9918). The ultraviolet absorbance spectra show increasing absorbances in the 270 nm region for the PE and EVA samples, matched by increasing infrared absorbances in the peroxide/hydroperoxide region. The stabilized EVA sample does not show this behaviour--there is no change in its IR spectrum, and its UV spectrum shows a decreasing absorbance at the wavelengths associated with the added UV stabilizers. Measurements of gel content of the exposed films, and of oxygen content of films at their point of failure provide ancillary information concerning changes in the films following exposure. Taken collectively, the observations are intended to serve as a basis for directing the development of computer models for polymer degradation.

II. Introduction

The overall goal of the Encapsulation Task of the Flat-Plate Solar Array Project is to identify and evaluate potential encapsulation materials for the protection of silicon solar cells. It is the task of the group headed by Dr. Guillet, at the University

of Toronto, to develop a computer program that simulates the kinetics of the ageing process of polymeric encapsulants. As sub-contractors to this group, our task has been to perform outdoor weathering and accelerated ageing studies on candidate polymer formulations. The experimental data obtained is to serve as a basis of comparison for the computer simulation experiments. In this report we document the materials studied, the ageing procedures used, and the analyses performed on the aged samples in order to provide this experimental background.

III. Experimental

The different elements of our experimental program can be outlined schematically as:

materials: choice of test pottant polymers → preparation of polymer films for testing → ageing procedures → analysis of aged samples

The chart below lists the relevant entries under these headings, each of which will be discussed.

Materials	Sample Preparation	Ageing Procedures	Analysis
EVA A9918 (Springboorn)	Crosslinked films, hot pressed to .004" thickness with peroxide crosslinkers.	Outdoor exposure (Toronto, south-facing 45° incidence)	Ultraviolet absorbance
ELVAX 150 (Dupont)			Infrared absorbance
PE UC4400 (Union Carbide)	Uncrosslinked films, hot pressed to .004" thickness with no crosslinkers present.	UV Accelerometer (American Ultraviolet)	elemental analysis gel/sol content
PS/MIPK actinometer (EcoPlastics)			actinometry

IIIa) Materials Tested

Our experimental testing program centered on the evaluation of one pottant material, an ethylene/vinyl acetate copolymer formulation developed by Springborn Labs[1.] and designated A9918. Other polymers tested served as a basis of comparison for this material.

EVA Formula A9918 was obtained from Springborn Labs as a 0.018" thick sheet of transparent, flexible, and slightly tacky polymer. It is made of an ethylene/vinyl acetate copolymer to which a crosslinking agent and UV stabilizers have been added. In its recommended use as a pottant, during encapsulation it is heated to crosslink the polymer. (The reader is referred to Springborn's own technical literature[1.] for a more complete discussion of the A9918 material.)

ELVAX 150 is a commercial Dupont copolymer of ethylene and vinyl acetate containing 20% vinyl acetate. This material is the base polymer for the A9918 formulation.

Polyethylene: A low density liner grade polyethylene supplied by Union Carbide, UC4400, was used as a control polymer for both the outdoor and accelerated ageing studies.

PS/MIPK Actinometer: As part of an earlier phase of this project, EcoPlastics developed a styrene/methylisopropenyl ketone copolymer for use as a chemical actinometer measuring solar intensity.[2.] The degradation of this polymer following solar exposure has been calibrated by monitoring its molecular weight change via high

precision automatic viscometry.[3.] This calibrated actinometer polymer was used throughout the ageing program to determine the exposure levels.

IIIb) Sample Preparation

A total of seven different series of polymer films was prepared:
1) EVA A9918 crosslinked
2) EVA A9918 uncrosslinked
3) (EVA A9918 + peroxide catalyst) crosslinked
4) ELVAX 150 uncrosslinked
5) (ELVAX 150 + peroxide catalyst) crosslinked
6) Polyethylene
7) PS/MIPK actinometer

1) EVA A9918 crosslinked

The A9918 film as received from Springborn is a 0.018" thick sheet, which proved to be too thick for the various spectroscopic analyses performed on the samples. The film was pressed between Teflon plates in a Carver press, heated to 150°C in order to activate the crosslinking agent in the material. Since this crosslinking process appears to result in gas evolution, the films were pressed at low pressure (3500 - 4000 psi) for five minutes to prevent bubble formation. Following this initial period, the films were pressed at a load pressure of 25000 psi for a further fifteen minutes to ensure complete crosslinking. The resultant films were 0.004" thick as

measured by a micrometer. (Care was taken with these tacky thin films that the faces of the micrometer were wetted to prevent binding of the films.) Strips of film about 2.5 x 7.5 mm were cut out and tape-mounted to slide holders for exposure testing.

2) EVA A9918 uncrosslinked

In order to obtain thin, uncrosslinked A9918 films for comparison with the crosslinked samples in 1), the pressing temperature was reduced to 85°C and pressing time limited for five minutes at 25000 psi. Since the crosslinker incorporated in the A9918 formulation is essentially inactive below 100°C, it is felt that these conditions are mild enough to ensure the preparation of an uncrosslinked thin film. Samples for exposure testing were prepared as in 1).

3) EVA A9918 + Lupersol 101 crosslinked

As a further test of the importance of crosslinking on the stability of the polymer, the A9918 formulation was modified by the addition of 1.5% w/w of additional crosslinker: Lupersol 101 (2.5-dimethyl-2, 5-di(t-butylperoxy) hexane; Pennwalt Corporation). The A9918 and the Lupersol 101 were first blended on a two-roll mill operating at 85°C--hot enough to facilitate blending but not to initiate crosslinking. A master batch of 10% w/w Lupersol was first produced; this was blended down to the 1.5% w/w final value and then pressed into a 0.004" thick film on the Carver press as in sample 1).

4) Elvax 150 uncrosslinked

Thin films of this EVA base polymer were prepared by pressing beads of the polymer (as it is supplied) at 130°C for approximately one minute at 25000 psi on the Carver press. Care was taken to ensure that the beads were heated to a malleable level before pressing was started.

5) Elvax 150 + Lupersol 101: crosslinked

This combination mimics the A9918 formulation with the difference that no UV stabilizer is present. Sample preparation was the same as for sample 3), substituting Elvax 150 for the A9918.

6) Polyethylene

Low density polyethylene films 0.003" thick were obtained readily by pressing pellets of UC4400 on the Carver press at 110°C and 20000 psi for approximately one minute. In contrast to the preceding EVA films, it was not necessary to use Teflon plates to facilitate film removal; instead Al foil-coated metal plates were adequate.

7) PS/MIPK actinometer

The actinometer polymer used was a styrene/methyl isopropenyl ketone copolymer containing 0.6% MIPK. Pellets of this polymer were pressed at 200 - 220°C, 20000 psi for approximately one minute, giving films of 0.008" thickness. (The thicker films were desirable since no spectroscopic measurements were to be made on them; rather the films were dissolved for viscometric measurements which benefitted from increased sample size.)

The various film samples are summarized in the chart below.

Sample	Thickness	UV Stabilizer	Crosslinker present in initial polymer	Crosslinker added to initial polymer	Sample crosslinked
1) EVA A9918 crosslinked	0.004"	✓	✓	✗	✓
2) EVA A9918 uncrosslinked	0.004"	✓	✓	✗	✗
3) EVA A9918 + Lupersol 101	0.004"	✓	✓	✓	✓
4) Elvax 150 uncrosslinked	0.004"	✗	✗	✗	✗
5) Elvax 150 crosslinked	0.004"	✗	✗	✓	✓
6) Polyethylene	0.003"	✗	✗	✗	✗
7) PS/HIPK	0.008"	✗	✗	✗	✗

IIIc) Ageing Procedures

The film samples described above were exposed, as duplicate samples, to both outdoor and accelerated ageing. Unexposed films were kept in the dark as controls. The outdoor exposures were made at Toronto, on an exposure rack on the roof of EcoPlastics' building facing south and inclined 45°C to the horizontal. Film samples were taken down at three week intervals and tested, at which time actinometer films were changed and the solar exposure over the three-week period determined. No attempt was made to control the sample temperatures which, since the exposure period covered most of one winter, were in the range of -10 to +10°C. [4] Exposure to an urban atmosphere resulted in some dust and soot accumulation particularly on the soft, tacky, EVA films. This does not, however, appear to have strongly influenced our spectroscopic data.

Accelerated ageing wasperformed on duplicate film samples using an American Ultraviolet accelerated ager. Sample films were placed 8" from a 1200 watt low pressure mercury lamp jacketed with Corex glass. Since this glass transmits light down to 280 nm, the radiation is slightly stronger in the 280-300 nm region relative to the solar spectrum. Samples were irradiated for 70 hour intervals, with spectroscopic analyses after each irradiation period. Duplicate actinometer films were analyzed after each interval to determine the equivalent solar exposure.

IIId) Analyses

The measurements performed can be grouped into two categories: 1) those performed after every exposure interval, either outdoor or in the accelerated ager, and designed to track in detail the changes in the films. These include the UV absorbance spectra, infrared absorbance spectre and the concommitant actinometry. The gel content analysis was performed on a less frequent basis, but still fits this category; 2) those performed on a before and after failure basis. The elemental analysis, specifically the oxygen content, falls in this category and is designed to measure the chemical changes evident at the point of failure.

Ultraviolet Spectroscopy

UV spectra were run on a Perkin Elmer Lambda 3 spectrometer, with a scan from 400 nm to 190 nm. Each sample film was run against an air reference with the absorbance at 400 nm, 327 nm, 287 nm and 270 nm, determined from the spectra. In addition, each film sample was run against an unexposed reference film as an alternative means of determining changes in the UV absorbance. This is particularly important at short wavelengths (215 -235 nm) where the absolute absorbance values are high. In all cases, care was taken to ensure that the films were positioned reproducibly in the spectrometer to minimize any effects of film inhomogeneity. For some of the highly degraded films, the physical distortion

of the sample necessitated some relaxation of this constraint.

Infrared Spectroscopy

Infrared spectra were recorded on a Bausch and Lomb Spectronic 250 spectrometer over the frequency range of 4000 - 650 cm^{-1}. Samples were run against an air reference; attempts to run spectra with unexposed films as references gave absorbance difference spectra that were not quantitatively consistent and hence were not used.

Actinometry

Irradiated actinometer films were cut into approximately 0.1g samples, weighed accurately and dissolved in 10 ml of toluene overnight. These solutions were filtered and the viscosity measured on an EcoPlastics Automatic Viscometer[3] at 30°C. From this solution viscosity, η, and that for pure toluene solvent, η_0, we calculate the intrinsic viscosity of the polymer from the Solomon-Cuita equation:

$$1) \qquad [\eta] = \left[\frac{(\eta_{sp}/c) - (\ln \eta_{rel}/c)}{0.5\ c} \right]^{1/2}$$

where $\eta_{rel} = \eta/\eta_0$, $\eta_{sp} = \eta_{rel} - 1$ and c is the polymer concentration in g/dl. The molecular weight of the polymer is calculate using the relationship[2]:

2) $[\eta] = 1.1 \times 10^{-4} \bar{M}_v^{0.725}$

The number of chain breaks per molecule is given by

3) $\#\text{ chain breaks} = \frac{\bar{M}_v(0)}{\bar{M}_v(t)} - 1$

where $\bar{M}_v(0)$ and $\bar{M}_v(t)$ are the polymer molecular weight before and after irradiation respectively. The number of chain breaks in the actinometer polymer is our measure of integrated solar intensity. From our earlier work[2], we have defined:

4) 1 Toronto Summer Day = 0.211 chain breaks/mol.

This relationship is used throughout to calculate the effective exposure levels of both outdoor and accelerated ageing samples.

Gel Content Determination

Exposed films of samples 1 - 5 of section III b were cut, weighed and placed in a 3.5 ml test tube to which 2 ml of toluene was added. The test tube was closed and heated in a water bath to 70°C for five hours. The contents were then filtered through pre-weighed No. 542 filter paper.* A second 2 ml aliquot of toluene was used to rinse the test tube; this too was filtered

* Beter results were obtained if the filter paper was pre-soaked in toluene and allowed to dry at room temperature to constant weight before use.

through the filter paper. After filtration, the filter paper, with any collected gel, was allowed to dry at room temperature overnight to constant weight. The % gel content is given by

5) $\%\text{ gel} = \frac{\text{wt of gel}}{\text{wt of film sample}} \times 100$

Oxygen Content Determination (Elemental Analysis)

Both unexposed films and exposed films at their point of failure (where possible) were sent to Guelph Chemical Lab. Ltd., Guelph, Ontario, for standard carbon and hydrogen content analysis. The oxygen content was calculated as the remainder.

IV. Results and Discussion

The accumulated effective solar exposure level, measured over the duration of both the outdoor and accelerated ageing experiments, are presented in Table 1 and Figure 1 for outdoor exposures, Table 2 and Figure 2 for accelerated exposure. Results are given as equivalent summer days as a function of actual exposure time. Not surprisingly, the plot for the accelerated ager results (Fig. 2) is nearly linear, reflecting the constancy of the exposure source. The outdoor results (Fig. 1) are however, also nearly linear, reflecting perhaps, the winter period over which the exposures were made.

The chart below outlines the tabular and graphic presentation of the UV absorbance data at the various exposure levels for each

of the seven samples discussed in section IIIb.

Sample	Crosslinked X Uncrosslinked O	Wavelength	Accelerated Ageing	Outdoor Ageing
			Table/Figure	Table/Figure
6) Polyethylene	O	400	3a	11c
6) Polyethylene	O	270	3b	12c
6) Polyethylene	C	210 (ΔAbs)	3b	13c
4) Elvax 150	O	400	4a	11a
5) Elvax 150	X	400	4b	11b
4) Elvax 150	O	270	5a	12a
5) Elvax 150	X	270	5b	12b
4) Elvax 150	O	210 (ΔAbs)	6a	13a
5) Elvax 150	X	210 (ΔAbs)	6b	13b
2) A1198	O	400	7a	14a
1) A9918	X	400	7b	14b
3) A9918+Lupersol 101	X	400	7c	14c
2) A9918	O	327	8a	15a
1) A9918	X	327	8b	15b
3) A9918+Lupersol 101	X	327	8c	15c
2) A9918	O	287	9a	16a
1) A9918	X	287	9b	16b
3) A9918+Lupersol 101	X	287	9c	16c
2) A9918	O	215 (ΔAbs)	10a	17a
1) A9918	X	215 (ΔAbs)	10b	17b
3) A9918+Lupersol 101	X	215 (ΔAbs)	10c	17c

Each figure shows the results for the duplicate samples tested, as well as for the unexposed control sample.* The tables give, in addition to the data for the figures, the slope and correlation coefficient for the best fit linear least squares line through the data.

Considering first the accelerated ageing results, at 400 nm the changes in the polyethylene and uncrosslinked and crosslinked Elvax 150 spectra (Figures 3a, 4a, and 4b respectively) are relatively small. The normal photo oxidation processes occurring in polymers are not expected to produce chromophores that absorb at this "control" wavelength; they are, however, expected to produce carbonyl moieties that will absorb in the 270 nm region. The absorbance changes at this wavelength (Fig. 3b for polyethylene, Fig. 5a and 5b for uncrosslinked and crosslinked Elvax 150) are indeed substantial, with the rate of change for the polyethylene sample being nearly 1.5x that for either the crosslinked or uncrosslinked Elvax 150 (slope m = +.0036 vs. m = +.0026). The same result holds true for the absorbance difference spectra (sample vs. unexposed reference) run at 210 nm. (Figures 3c, 6a, and 6b): there is no difference between crosslinked and uncrosslinked Elvax 150, both of which give an absorbance change 1.5x slower than polyethylene (m = +.029 vs. m = +.019).

*Subsequent to the measurements discussed here, a separate set of controls kept in the dark but at 40°C (the accelerated ager temperature) were run. These controls gave the same results at those used here. Results are given in Appendix A.

The spectra for the preceding three samples are relatively featureless: the polyethylene shows an absorbance increasing roughly inversely proportional to wavelength due to light scattering; the Elvax 150 gives a similar curve upon which is superimposed a weak ester carbonyl band (from the vinyl acetate) in the 270 nm region. The A9918 samples are quite different, however, showing strong absorbance maxima at 327 nm and 287 nm due to the added UV stabilizers. At 400 nm, the changes in absorbance for uncrosslinked (Fig. 7a), crosslinked (Fig. 7b), and crosslinked with added Lupersol 101 (Fig. 7c) A9918 polymer are all small. The exposed samples may show a slight decrease, with the unexposed references showing a comparably small increase, but both effects are close to the experimental error limits. At 327 nm (Figures 8a-c) and 287 nm (Figures 9a-c) there are pronounced decreases in the absorbance of the exposed samples, with the unexposed reference samples consistently showing a small increase. The decrease in the 327 nm and 287 nm absorbances is attributed to loss or destruction of the added UV stabilizers as the sample ages. At neither wavelength is there a significant difference in the rate of change in comparing the uncrosslinked sample ($m = -.0024$ at 327, $m = -.0017$ at 287) with either of the crosslinked ones ($m = -0.0027$ at 327, $m = -0.0018$ at 287). In comparing the rates of change at 327 and 287 nm, since the absorbance is higher at the shorter wavelength, one would expect a greater absolute change in the absorbance there than at the

longer wavelength if both bands are due to the same absorber. That the rate of decrease of the 287 nm band is in fact slightly lower than that of the 327 nm band may indicate two UV absorbers being consumed at different rates. It may, however, also be due to an increasing carbonyl absorbance at the shorter wavelength (viz. the 270 nm data for Elvax 150 above) partially offsetting the decrease in the UV stabilizer absorption band. The results at 210 nm (absorbance difference spectra, Figures 10a-c) tend to support the latter explanation. Following an initial decrease, the absorbance starts to increase sharply (the slopes given in the Tables are for this latter region). No quantitative explanation is attempted, but qualitatively a rapidly increasing strong absorbance, such as that shown at this wavelength for the Elvax 150 samples, superimposed on a declining UV stabilizer absorbance, with a lower rate of change, would give rise to this type of curve.

The outdoor exposures are, at this stage, too low to provide much useful information regarding the breakdown of the test polymers. Figures 11a-c demonstrate a problem common to all outdoor weathering experiments: at 400 nm where little change in the UV absorbance is expected, exposed polyethylene and Elvax 150 samples (crosslinked and uncrosslinked) show an increase in "absorbance", presumably due to dust and dirt accumulation and surface roughening. This increase is large—slope $m = +0.018$—and, if evident at other wavelengths, would tend to swamp the smaller changes expected from polymer photo degradation.

This is borne out for the polyethylene and Elvax samples at 270 nm (Fig. 12a-c) for which the apparent UV absorbance increases are much larger than for the accelerated ageing runs (m = +.024 vs. m = +.0026 for Elvax 150, m = +.014 vs. +.0036 for PE). At 210 nm the absorbance changes are sufficiently large that this background effect is less important; nonetheless the changes for Elvax 150 (Fig. 13a, b; m = +.022 vs. m = +.019 for the accelerated ager) and for polyethylene (Fig. 13a; m = +.028 outdoor vs. m = +.029 accelerated ageing) are made difficult to interpret.

This comment is also valid with respect to the various A9918 films, results for which are presented in Figures 14-17. Whereas for the accelerated ager the major observation was the apparent decrease in UV stabilizer absorbance, here all samples at all wavelengths measured show an increase in absorbance. This increase is present even at 400 nm and has a slope similar to those observed for the polyethylene and Elvax samples at 400 nm (m +.010). This rate of increase is substantially larger than the changes observed in the accelerated ageing runs and prevents any meaningful interpretation of these results. It must be noted that the exposure range covered in the outdoor tests spans less than the first two data points in the accelerated ager experiments. Longer outdoor exposures may start to show the trends evident from the accelerated degradation, but at all times care must be exercised to account for nondegradative weathering effects.

The infrared spectra provide results that complement the

above UV data. Since the A9918 and Elvax 150 polymers contain acetate groups, the conventional carbonyl index analysis was not feasible. (With a higher resolution IR spectrometer it may be possible to separate acetate vs. ketone carbonyl bands well enough to permit such an analysis; with our current equipment such attempts were unsuccessful). Instead, we have analyzed the 3500-3100 cm^{-1} region wherein we expect absorbances due to hydroxide, carboxylic acid, hydroperoxide and peroxide groups. Results for Elvax 150 uncrosslinked and crosslinked and for polyethylene are given in Figures 18a-c and Table 18 a-c respectively for accelerated ager exposures. For all three samples, an increase in absorbance with exposure time was evident over the entire 3500-3100 cm^{-1} range. The actual measurement was made at 3100 cm^{-1} since the peroxide and hydroperoxide absorbance bands, potentially present due to degradation, are expected in this region. There is little difference between crosslinked and uncrosslinked Elvax 150, with both giving results close to those for polyethylene. All three samples show slight evidence for an increase in the rate of absorbance change with increasing exposure. The most striking difference, however, comes from comparing these results with those for the A9918 samples. None of the A9918 samples show any change in the aborbance in the 3500-3100 cm^{-1} region within our measurement limits. The most attractive explanation of this observation relies on the UV absorbance results also. The decrease in UV absorbance at 327 nm and 287 nm for the A9918 samples was attributed to loss or consumption

of the added UV stabilizers. The consumption of these stabilizers does in fact provide the stabilization expected: by sacrificing the stabilizers, the formation of polymer degradation products is stopped, as evidenced by the IR data.

The gel content analysis results, presented in Table 19 and Figure 19, add a further complementary observation to those above: uncrosslinked EVA films (Elvax 150) do not crosslink upon exposure; crosslinked EVA films (A9918) do not disintegrate upon exposure. The data are primarily from the accelerated ager tests. Within the exposure limits tested, there appears to be insufficient chain degradation of the A9918 to break down the gel.

Our final analysis, that of oxygen content, differs from the preceding analyses in that it was performed only on unexposed samples and on samples at their failure point. This failure point is defined as the brittleness point for polyethylene (based on a 180° fold test); it is harder to define for the various EVA samples.

For Elvax 150 samples, the point of failure was (arbitrarily) set as the point at which the film deformed sufficiently to prevent any further use in the spectroscopic measurements. For the A9918 samples, it was the maximum exposure level in the accelerated ageing tests. Results are given in Table 20.

Polyethylene shows an increase in oxygen content with exposure level, going from 0.13 to 4.48% at point of failure (105 Summer Days exposure). Elvax 150, uncrosslinked, failed after 100 Summer Days, showing a 5.37% increase in oxygen content. The crosslinked Elvax 150 failed slightly later (110 Summer Days) and showed a

higher oxygen content at point of failure (oxygen gain = 8.10%). Once again, the A9918 samples behave quite differently. At the maximum exposure level there is no increase in oxygen content for either crosslinked or uncrosslinked samples. This correleates well with the IR results which also suggested no oxygen uptake.

The preceding data, taken collectively for the various analyses performed, should serve as a framework to guide the development of computer modelling studies. This is particularly true for the polyethylene and Elvax 150 samples since they are not affected by the presence of added stabilizers as are the A9918 materials. The overall stability of the A9918 samples with respect to all others is clearly apparent, although the consumption of the UV stabilizers will ultimately lead to failure as for the Elvax 150 material. It is interesting to calculate the point at which the UV absorbance due to the stabilizers will be reduced to zero. Assuming that we can simply extrapolate our data, using the 327 nm results for A9918 we obtain values of 370 Summer Days for the crosslinked samples, 450 Summer Days for the uncrosslinked. (It is possible that the crosslinking agent consumers some of the stabilizer). No calibration has been made to determine the number of Summer Days in a calendar year; however, if we assume a value of 75 Summer Days = 1 year, then degradation of the A9918 material may begin in the five-year range.

References

1. T. B. Baum and P. Willis, A9918 Technical Information Packet, Springborn Laboratories.

2. Modelling of Photodegradation in Solar Cell Modules, Annual Report, EcoPlastics, 1980.

3. a) T. Kilp, B. Bouvenaghel-Defoort, W. Penning and J. E. Guillet, Rev. Sci. Instrum., 47, 1496 (1976).
b) M. Breton, J. Poly. Sci, Poly. Phys., 21, 1559 (1983).

4. a) Monthly Radiation Summary, Environment Canada, Vol. 24 (1983), Vol. 25 (1984).
b) Monthly Meteorological Summary, Environment Canada, (Lester B. Pearson International Airport), monthly summaries for Nov. 1983 - Feb. 1984.

Appendix A.

To ensure that thermal degradation alone was not responsible for the UV absorbance changes observed in the accelerated ager samples, a series of heated (40°C) dark controls of crosslinked A9918 were run. Results are presented in Table A1 and plotted in Figures A1 and A2 as UV absorbance at 400 nm, 327 nm, 287 nm and 215 nm vs. days of heating. The 21 days of heating correspond to 500 hours in the accelerated ager. The lack of any significant change in UV absorbance at any of the wavelengths measured demonstrates the validity of our assumption of little thermal contribution to the observed photo-degradations.

Table A1 UV absorbance changes of cross-linked EVA (A9918) with heating time at 40°C without irradiation

Heating Time	Abs. at 400 nm		Abs. at 427 nm		Abs. at 287 nm		Abs. difference at 219 nm
# of Days	unheated ref.	heated sample film	unheated ref.	heated film	unheated ref.	heated film	heated film unheated ref.
0	0.240	0.308	0.847	1.261	1.262	1.749	1.828
3	0.251	0.290	0.868	1.234	1.293	1.720	1.754
10	0.253	0.286	0.871	1.221	1.293	1.702	1.734
14	0.252	0.287	0.868	1.217	1.294	1.699	1.693
18	0.254	0.288	0.871	1.216	1.297	1.704	1.742
21	0.252	0.285	0.869	1.211	1.296	1.693	1.755

Table 1 Equivalent Toronto Summer Days calculated for outdoor exposures (Nov. 15, 1983 to Feb. 24, 1984)

Date	Exposure Time		[η]	M_v	No. of chain breaks	Toronto Summer Days	
	Weeks	Total			M_{v0}/M_v^{-1}	Period	Total
Unexposed	0	0	0.712	1.806×10^5	0	0	0
Nov.14–Nov.29 1983 1983	2	2	0.6629	1.633×10^5	0.1063	0.504	0.504
Nov.30–Dec.21 1983 1983	3	5	0.5313	1.206×10^5	0.4975	2.358	2.862
Dec.23–Jan.13 1983 1984	3	8	0.5315	1.179×10^5	0.5318	2.529	5.3824
Jan.14–Feb.3 1984 1984	3	11	0.5464	1.253×10^5	0.4413	2.092	7.474
Feb.3–Feb.24 1984 1984	3	14	0.5167	1.161×10^5	0.5556	2.633	10.107

Table 2 Equivalent Toronto Summer Days calculated for the accelerated ager ...ing the Actinometer films H-63

Irradiation Time Hours	Total Hrs	Int. visc	M_v	No. of chain breaks M_v/M_v^{-1}	Toronto Summer Days Period	Total
0	0	0.712	1.806×10^5	0	0	0
70	70	0.3056	5.624×10^4	2.2112	10.480	10.480
70	140	0.3333	6.3392×10^4	1.8489	8.763	19.243
70	210	0.3025	5.5457×10^4	2.2566	10.695	29.938
70	280	0.3383	6.4697×10^4	1.7915	8.490	38.428
70	350	0.3245	6.109×10^4	1.9563	9.271	47.699
70	420	0.3208	6.690×10^4	2.1740	10.303	.02
70	490	0.3335	6.328×10^4	1.8540	8.7866	66.789
70	560	0.3321	6.308×10^4	1.8630	8.8295	75.618
70	630	0.3082	6.012×10^4	2.0040	9.4976	85.116
70	700	0.3696	6.464×10^4	1.4196	6.7280	91.844
70	770	0.3392	6.694×10^4	1.6979	8.0470	99.891
70	840	0.4020	8.368×10^4	1.1582	5.4890	105.38
70	910	0.3180	5.941×10^4	2.0399	9.6677	115.048
70	980	0.3291	6.442×10^4	1.8035	8.5473	123.595
70	1050	0.3089	6.218×10^4	1.9045	9.026	132.621
130	1180	0.3068	5.709×10^4	2.1634	10.253	142.874

Table 1a Ultra-violet absorbance changes of low density Polyethylene film with irradiation time in accelerated ager

Irradiation Time Toronto Summer Days	UV absorbance at 400 nm Film Samples Polyethylene (low density) Unexposed # 812	Duplicates # 303	# 304
0	0.450	0.489	0.396
10.48	0.432	0.469	0.395
19.243	0.434	0.477	0.398
29.938	0.436	0.481	0.402
38.428	0.435	0.481	0.407
47.699	0.436	0.493	0.412
58.002	0.435	0.499	0.417
66.789	0.426	0.505	0.426
75.618	0.436	0.510	0.429
85.116	0.438	0.519	0.435
91.844	0.447	0.540	0.449
99.891	0.438	0.541	0.451
105.38	0.438	0.555	0.456 (broken)
115.048	0.437	0.559	–
123.595	0.437	0.569	–
132.621	0.438	0.578	–
142.891	–	–	–
Slope m correlation	0 0.02423	0.0008 0.98494	0.0007 0.9862
Δ aba$_{105}$	0.006	0.082	0.061

Table 3b Ultra-violet absorbance changes of low density Polyethylene film with irradiation time in accelerated ager

Irradiation Time Toronto Summer Days	UV absorbance at 170 nm Film Samples Polyethylene (low density)		
	Unexposed	Duplicates	
	# 312	# 303	# 304
0	0.561	0.624	0.504
10.48	0.570	0.639	0.546
19.243	0.561	0.648	0.552
29.938	0.567	0.6825	0.585
38.428	0.564	0.7125	0.609
47.699	0.563	0.756	0.633
58.002	0.561	0.795	0.666
66.789	0.561	0.825	0.6975
75.618	0.563	0.852	0.72
85.116	0.557	0.888	0.75
91.844	0.579	0.953	0.81
99.891	0.570	0.954	0.819
105.38	0.567	1.002	0.832 (broken)
115.048	0.570	1.095	-
123.595	0.563	1.128	-
132.621	0.564	1.16	-
142.891	0.567	1.236	-
Slope m	0	0.0044	0.0028
correlation	0.30662	0.98573	0.96092
Δabs_{105}	0.006	0.378	0.328

Table 3c Absorbance difference (at maxima) for low density Polyethylene film with increase in accelerated ager exposure time

Irradiation Time Toronto Summer Days	UV absorbance difference at 210-220 nm Film Samples Polyethylene (low density)	
	Duplicates	
	# 303	# 304
0	0.3831	0.2417
10.48	0.492	0.6603
19.243	0.6603	0.6273
29.938	0.723	0.7065
38.428	1.1685	1.108
47.699	1.3533	1.2081
58.002	1.8054	1.6371
66.789	2.1486	1.9308
75.618	2.472	2.2196
85.116	2.7905	2.4984
91.844	3.100	2.8482
99.891	3.235	2.947
105.38	3.369	3.076 (broken)
115.048	-	-
123.595	3.361	-
132.621	4.214	-
142.891	4.214	-
Slope m	0.0294	0.0288
correlation	0.98909	0.99351
Δabs_{105}	2.986	2.835

Table 4 (a, b) Ultra-violet absorbance changes of (a) uncross-linked and (b) cross-linked Elvax 150 films with irradiation time in accelerated ager

Irradiation Time Toronto Summer Days	UV absorbance at 400 nm: Film Samples Elvax 150 uncross-linked Unexposed # R219	Duplicates # 54	# 59	Film Samples Elvax 150 cross-linked Unexposed # R83	Duplicates # 40	# 58A
0	0.216	0.261	0.294	0.240	0.276	0.264
10.48	0.212	0.190	0.185	0.287	0.195	0.187
19.243	0.213	0.181	0.178	0.285	0.185	0.175
29.938	0.222	0.183	0.180	0.292	0.184	0.173
38.428	0.221	0.185	0.184	0.293	0.183	0.170
47.699	0.223	0.181	0.194	0.290	0.167	0.177
58.002	0.224	0.180	0.189	0.294	0.179	0.167
66.789	0.223	0.181	0.181	0.294	0.164	0.159
75.618	0.223	0.177	0.174	0.293	0.162	0.146
85.116	0.216	0.165	0.167	0.293	0.142	0.136
91.844	0.231	0.152	0.140	0.301	0.130	0.130
99.891	0.231	0.139	0.140	0.299	0.117	0.126
105.38	0.228	0.137	0.127	0.298	0.104	0.118
115.048	0.228	0.131	0.128	0.297	0.111	deformed
123.595	0.220	0.156	0.143	0.289	0.106	
132.621	0.226	0.180	0.137	0.299	0.119	
142.891						
Slope m	0.0001	-0.0004	-0.0005	0.0002	-0.001	-0.0009
correlation	0.67578	-0.69687	-0.74461	0.61062	-0.91275	-0.88546

Table 5 (a, b) Ultra-violet absorbance changes of (a) uncross-linked and (b) cross-linked Elvax 150 films with irradiation time in accelerated ager

Irradiation Time Toronto Summer Days	UV absorbance at 270 nm: Film Samples Elvax 150 uncross-linked Unexposed # R219	Duplicates # 54	# 59	Film Samples Elvax 150 cross-linked Unexposed # R83	Duplicates # 40	# 58A
0	0.342	0.345	0.387	0.456	0.420	0.450
10.48	0.321	0.251	0.240	0.469	0.309	0.317
19.243	0.342	0.258	0.255	0.476	0.319	0.327
29.938	0.348	0.276	0.276	0.489	0.341	0.351
38.428	0.341	0.306	0.306	0.489	0.370	0.361
47.699	0.360	0.330	0.330	0.495	0.408	0.405
58.002	0.363	0.375	0.375	0.492	0.438	0.432
66.789	0.360	0.396	0.396	0.492	0.441	0.447
75.618	0.367	0.416	0.419	0.495	0.459	0.465
85.116	0.358	0.420	0.428	0.498	0.462	0.471
91.844	0.378	0.435	0.444	0.504	0.495	0.501
99.891	0.370	0.413	0.445	-	-	-
105.38	0.372	0.456	0.466	0.501	0.484	0.593 (failed)
115.048	0.376	0.493	0.570	0.502	0.553	
123.595	0.364	0.526	0.588	0.491	0.569	
132.621	0.375	0.607	0.637	0.504	0.725	
142.891						
Slope m	0.0003	0.0026	0.0027	0.0003	0.0031	0.0024
correlation	0.8	0.90069	0.91599	0.85379	0.92284	0.99257
Δabs_{105}	0.051	0.205	0.226	0.032	0.175	0.226

Table 6 (a, b) Changes of ultra-violet absorbance of (a) uncross-linked and (b) cross-linked Elvax 150 films with irradiation time in accelerated ager

Irradiation Time Toronto Summer Days	UV absorbance difference at 215-235 nm			
	Film Samples Elvax 150 uncross-linked Duplicates		Film Samples Elvax 150 cross-linked Duplicates	
	# 54/R219	# 59/R219	# 40/R83	# 58A/R83
0	-0.2241	-0.1383	-0.135	0.047
10.48	-0.2954	-0.2894	<-0.3	-0.102
19.243	-0.295	-0.135	-0.211	-0.006
29.938	-0.2109	-0.0459	-0.036	0.212
38.428	-0.0904	0.096	0.183	0.446
47.699	0.0795	0.261	0.334	0.624
58.002	0.268	0.4421	0.584	0.829
66.789	0.4755	0.6768	0.716	0.987
75.618	0.6801	0.8418	0.779	1.093
85.116	0.921	0.9953	0.990	1.271
91.844	1.1025	1.2609	-	1.350
99.891	-	1.3236	1.0926	1.436
105.38	1.251	1.5513	-	1.5563
115.048	-	-	-	-
123.595	-	-	-	-
132.621	-	1.9688	2.0595	-
142.891	-	-	-	-
Slope m correlation	0.0196 0.99276	0.0193 0.99534	0.0188 0.98986	0.0178 0.99577
$\Delta_{abs_{105}}$	1.841	1.546	1.658	-

Table 7 (a, b) UV absorbance changes of (a) uncross-linked and (b) cross-linked EVA (Formula A9918) with irradiation time in accelerated ager

Irradiation Time Toronto Summer Days	UV absorbance at 400 nm					
	Film Samples EVA A9918 uncross-linked			Film Samples EVA A9918 cross-linked		
	Unexposed	Duplicates		Unexposed	Duplicates	
	# R213	# 93	# 9	# R45A	# 208	# 76
0	0.246	0.189	0.258	0.240	0.261	0.273
10.48	0.251	0.149	0.240	0.252	0.255	0.277
19.243	0.254	0.152	0.212	0.252	0.253	0.272
29.938	0.272	0.148	0.225	0.260	0.247	0.263
38.428	0.277	0.147	0.226	0.263	0.244	0.257
47.699	0.289	0.145	0.225	0.272	0.240	0.255
58.002	0.299	0.140	0.220	0.273	0.235	0.252
66.789	0.314	0.138	0.223	0.276	0.234	0.245
75.618	0.324	0.136	0.225	0.279	0.234	0.264
85.116	0.340	0.134	0.221	0.286	0.235	0.260
91.844	0.353	0.131	0.240	0.295	0.236	0.260
99.891	0.353	0.141	0.231	0.283	0.229	0.257
105.38	0.351	0.138	0.230	0.283	0.228	0.254
115.048	0.351	0.139	0.230	0.285	0.227	0.255
123.595	0.343	0.129	0.219	0.285	0.225	0.251
132.621	0.351	0.139	0.235	0.285	0.224	0.248
142.891	0.355	0.139	0.237	0.285	0.224	0.247
Slope m correlation	0.0005 0.95615	-0.0002 -0.69006	0 -0.09352	0.00 0.89469	-0.0002 -0.96056	-0.0002 -0.75189

Table 7c UV absorbance changes of cross-linked EVA (Formula A9918 with added Lupersol 101) with irradiation time in accelerated ager

Irradiation Time Toronto Summer Days	UV absorbance at 400 nm Film Samples EVA A9918 + catalyst cross-linked		
	Unexposed	Duplicates	
	# RST2	# 35	# ST
0	0.249	0.201	0.375
10.48	0.245	0.138	0.332
19.243	0.252	0.136	0.312
29.938	0.255	0.133	0.306
38.428	0.255	0.132	0.304
47.699	0.260	0.136	0.301
58.002	0.257	0.134	0.296
66.789	0.260	0.133	0.292
75.618	0.261	0.135	0.293
85.116	0.262	0.136	0.291
91.844	0.270	0.142	0.296
99.891	0.261	0.135	0.289
105.38	0.264	0.134	0.288
115.048	0.264	0.115	0.285
123.595	0.258	0.131	0.279
132.621	0.265	0.136	0.279
142.891	0.263	0.187	0.277
Slope m	0.0001	0	-0.0004
correlation	0.80617	0.02833	-0.83013

Table 8 (a, b) UV absorbance changes of (a) uncross-linked and (b) cross-linked EVA (Formula A9918) with irradiation time in accelerated ager

Irradiation Time Toronto Summer Days	UV absorbance at 327 nm Film Samples EVA A9918 uncross-linked			Film Samples EVA A9918 cross-linked		
	Unexposed	Duplicates		Unexposed	Duplicates	
	# R213	# 93	# 99	# R45A	# 208	# 76
0	0.933	1.080	1.050	0.789	1.068	1.200
10.48	0.936	1.030	0.998	0.800	1.024	1.167
19.243	0.952	1.033	0.996	0.[illegible]	1.009	1.148
29.938	0.968	1.012	0.979	0.819	0.987	1.117
38.428	0.976	0.994	0.966	0.812	0.971	1.089
47.699	0.996	0.964	0.947	0.833	0.945	1.056
58.002	1.011	0.931	0.921	0.830	0.923	1.022
66.789	1.033	0.900	0.899	0.846	0.891	0.981
75.618	1.047	0.870	0.881	0.846	0.869	0.966
85.116	1.073	0.845	0.872	0.862	0.839	0.924
91.844	1.095	0.824	0.868	0.872	0.824	0.892
99.891	1.092	0.814	0.834	0.855	0.790	0.870
105.38	1.095	0.787	0.814	0.853	0.769	0.841
115.048	1.094	0.768	0.793	0.862	0.744	0.810
123.595	1.081	0.736	0.763	0.854	0.727	0.786
132.621	1.094	0.735	0.765	0.873	0.705	0.757
142.891	1.098	0.704	0.737	0.867	0.773	0.718
Slope m	0.0014	-0.0027	-0.0021	0.0006	-0.0028	-0.0034
correlation	0.95911	-0.99616	-0.99449	0.98207	0.99792	-0.99881

Table 8c UV absorbance changes of cross-linked EVA (Formula A9918 with added Lupersol 101)with irradiation time in accelerated ager

Irradiation Time Toronto Summer Days	UV absorbance at 327 nm Film Samples EVA A9918 + catalyst cross-linked Unexposed # RST2	Duplicates # 35	# ST
0	0.629	0.852	1.002
10.48	0.747	0.800	0.916
19.243	0.750	0.761	0.877
29.938	0.755	0.751	0.860
38.428	0.756	0.733	0.836
47.699	0.757	0.718	0.820
58.002	0.759	0.697	0.796
66.789	0.759	0.676	0.769
75.618	0.752	0.657	0.757
85.116	0.810	0.640	0.729
91.844	0.781	0.624	0.730
99.891	0.762	0.596	0.706
105.38	0.758	0.577	0.689
115.048	0.749	0.559	0.671
123.595	0.747	0.545	0.651
132.621	0.763	0.531	0.637
142.891	0.760	0.503	0.616
Slope m	0.0004	-0.0023	-0.0024
correlation	0.45867	-0.99536	-0.98575

Table 9 (a, b) UV absorbance changes of (a) uncross-linked and (b) cross-linked EVA (Formula A9918) with irradiation time in accelerated ager

Irradiation Time Toronto Summer Days	UV absorbance at 287 nm Film Samples EVA A9918 uncross-linked Unexposed # R213	Duplicates # 93	# 99	Film Samples EVA A9918 cross-linked Unexposed # R45A	Duplicates # 208	# 76
0	1.326	1.599	1.425	1.092	1.596	1.770
10.48	1.324	1.513	1.374	1.110	1.598	1.723
19.243	1.326	1.527	1.370	1.109	1.565	1.693
29.938	1.363	1.494	1.342	1.128	1.541	1.652
38.428	1.373	1.470	1.327	1.114	1.572	1.616
47.699	1.404	1.436	1.312	1.152	1.487	1.589
58.002	1.422	1.399	1.290	1.148	1.462	1.564
66.789	1.447	1.371	1.270	1.172	1.423	1.545
75.618	1.468	1.349	1.261	1.171	1.405	1.560
85.116	1.490	1.328	1.273	1.191	1.349	1.536
91.844	1.517	1.330	1.269	1.200	1.357	1.545
99.891	1.516	1.334	1.245	1.180	1.346	1.550
105.38	1.522	1.330	1.232	1.178	1.313	1.534
115.048	1.532	1.333	1.233	1.196	1.310	1.572
123.595	1.509	1.317	1.203	1.179	1.307	1.578
132.621	1.524	1.335	1.220	1.206	1.322	1.573
142.891	1.527	1.322	1.211	1.194	1.292	1.619
Slope m	0.0017	-0.0019	-0.0014	0.0008	-0.0024	-0.0011
correlation	0.96122	0.96122	-0.96771	0.92585	-0.97775	-0.70436

Table 9c UV absorbance changes of cross-linked EVA (Formula A9918) with added Lupersol 101, with irradiation time in accelerated ager

Irradiation Time Toronto Summer Days	UV absorbance at 287 nm Film Samples EVA A9918 + catalyst cross-linked Unexposed Duplicates		
	# RST2	# 3S	# 8T
0	1.050	1.229	1.425
10.48	1.084	1.115	1.301
19.243	1.081	1.092	1.259
29.938	1.081	1.077	1.225
38.428	1.080	1.053	1.192
47.699	1.082	1.037	1.178
58.002	1.088	1.017	1.152
66.789	1.085	0.999	1.127
75.618	1.082	0.987	1.114
85.116	1.174	0.974	1.076
91.844	1.113	0.980	1.085
99.891	1.090	0.956	1.066
105.38	1.076	0.944	1.053
115.048	1.065	0.967	1.047
123.595	1.063	0.974	1.029
132.621	1.089	0.967	1.025
142.891	1.083	0.956	1.018
Slope m	0.0001	-0.0015	-0.0024
correlation	0.15092	-0.88647	-0.94852

Table 10 (a, b) Changes of UV absorbance of (a) uncross-linked and (b) cross-linked EVA (Formula A9918) with irradiation time in accelerated ager

Irradiation Time Toronto Summer Days	UV absorbance difference at 215-230 nm Film Samples EVA A9918 uncross-linked Duplicates		Film Samples EVA A9918 cross-linked Duplicates	
	# 93/R213	# 99/R211	# 76/R45A	# 208/R45A
0	0.2709	0.063	0.9639	0.581
10.48	0.2742	0.063	1.0624	1.350
19.243	0.3072	0.063	1.1454	1.4259
29.938	0.294	0.0861	1.0794	1.234
38.428	0.3103	0.1191	1.0365	1.185
47.699	0.3452	0.1752	1.1256	1.2098
58.002	0.4425	0.3039	1.2626	1.2609
66.789	0.5547	0.4029	1.2510	1.1256
75.618	0.492	0.3501	1.5183	1.3137
85.116	0.6834	0.6348	1.647	1.3642
91.844	0.7065	0.5976	1.7873	1.3599
99.891	0.8748	0.7775	1.8879	1.4127
105.38	0.8715	0.7395	1.9935	1.416
115.048	1.053	1.0332	2.0826	1.482
123.595	1.0332	0.9375	2.1882	1.6206
132.621	1.185	1.1025	2.2608	1.6569
142.891	1.218	1.218	2.4093	1.7625
Slope m	0.0074	0.0088	0.0143	0.0076
correlation	0.96347	0.96833	0.98658	0.97788

Table 10c Changes of UV absorbance of cross-linked EVA (Formula A9318 with added Luperaol 101) with irradiation time in accelerated ager

Irradiation Time Toronto Summer Days	UV absorbance difference at 215-230 nm Film Samples EVA A9918 + catalyst cross-linked Duplicates # ST/HST2	# 35/HST2
0	0.624	0.1554
10.48	0.4854	0.2148
19.243	0.426	0.1488
29.938	0.4161	0.1455
38.428	0.426	0.1752
47.699	0.4299	0.195
58.002	0.4359	0.2049
66.789	0.4359	0.2049
75.618	0.4458	0.2049
85.116	0.4343	0.2445
91.844	0.4953	0.261
99.891	0.5349	0.2841
105.38	0.657	0.4293
115.048	0.723	0.4986
123.595	0.7791	0.6438
132.621	0.7969	0.7395
142.891	1.0134	0.9392
Slope m	0.0092	0.0123
correlation	0.97944	0.98251

slope started from 85.116 summer days

Table 11 (a, b, c) UV absorbance changes of (a) uncross-linked and (b) cross-linked ELVAX 150 films and (c) low density Polyethylene films with outdoor exposure time

Outdoor Exposure Toronto Summer Days	UV absorbance at 400 nm Film Samples ELVAX 150 uncross-linked Unexposed # R219	Duplicates # 86	# 223	Film Samples ELVAX 150 cross-linked Unexposed # R83	Duplicates # R62	# 47	Film Samples Polyethylene (low density) Unexposed # R12	# 84	# 167
0	0.216	0.348	0.300	0.240	0.321	0.321	0.412	0.480	0.462
0.506	0.218	0.273	0.317	0.292	0.274	0.326	0.436	0.495	0.477
2.862	0.226	0.302	0.334	0.292	0.304	0.342	0.436	0.502	0 .488
5.3824	0.226	0.336	0.371	0.298	0.343	0.381	0.443	0.551	0.508
7.474	0.224	0.363	0.399	0.302	0.379	0.429	0.440	0.535	0.514
10.107	0.220	0.393	0.430	0.301	0.417	0.447	0.439	0.552	0.333
Slope m	0.0004	0.0125	0.0125	0.0012	0.0151	0.0133	0.0004	0.007	0.0068
Correlation	0.40356	0.99953	0.9962	0.91802	0.99901	0.98615	0.54377	0.90896	0.98589

Table 12 (a, b, c) UV absorbance changes of (a) uncross-linked and (b) cross-linked ELVAX 150 films and (c) low density Polyethylene films with outdoor exposure time

	UV absorbance at 270 nm								
Outdoor Exposure	Film Samples			Film Samples			Film Samples		
Toronto Summer Days	ELVAX 150 uncross-linked			ELVAX 150 cross-linked			Polyethylene (low density)		
	Unexposed	Duplicates		Unexposed	Duplicates		Unexposed	Duplicates	
	# R219	# 86	# 223	# R83	# R62	# 47	# R12	# 84	# 167
0	0.339	0.420	0.465	0.441	0.498	0.504	0.563	0.609	0.591
0.506	0.339	0.381	0.471	0.489	0.450	0.510	0.570	0.6495	0.630
2.862	0.3675	0.45	0.534	0.501	0.528	0.579	0.575	0.672	0.660
5.3824	0.369	0.497	0.597	0.507	0.558	0.609	0.576	0.744	0.687
7.474	0.369	0.561	0.627	0.501	0.642	0.705	0.564	0.735	0.708
10.107	0.372	0.613	0.677	0.504	0.690	0.730	0.568	0.767	0.747
Slope m	0.0033	0.0241	0.0215	0.0013	0.0248	0.0236	0.0001	0.0147	0.0137
Correlation	0.84999	0.99716	0.99546	0.70191	0.98923	0.97974	0.07131	0.94786	0.97796

Table 13 (a, b, c) Changes of UV absorbance of (a) uncross-linked and (b) cross-linked ELVAX 150 films and (c) low density Polyethylene films with outdoor exposure time

	UV absorbance difference at 210-220 nm					
Outdoor Exposure	Film Samples		Film Samples		Film Samples	
Toronto Summer Days	ELVAX 150 uncross-linked		ELVAX 150 cross-linked		Polyethylene (low density)	
	Duplicates		Duplicates		Duplicates	
	# 86/R219	# 223/R219	# 62/R83	# 47/R83	# 84/R12	# 167/R12
0	0.4145	0.096	0.0416	-0.1581	0.063	0.027
0.506	0.261	0.096	-	-	0.129	0.096
2.862	0.327	0.1950	-	-0.1251	0.2016	0.1719
5.3824	0.3798	0.3039	-	-0.168	0.3056	0.2049
7.474	0.525	0.3501	-0.267	0.0366	0.3122	0.2742
10.107	0.558	0.393	-0.135	0.2346	0.3699	0.327
Slope m	0.033	0.0314	0.0501	0.0848	0.0288	0.0271
Correlation	0.9753	0.97893	1.0	0.99715	0.96503	0.97678

Table 14 (a, b, c) UV absorbance changes of (a) uncross-linked and (b)cross-linked EVA (Formula A9918) and (c) cross-linked EVA (Formula A9918 + Lupersol 101) films with outdoor exposure time

UV absorbance at 400 nm

Outdoor Exposure	Film Samples			Film Samples			Film Samples		
Toronto Summer Days	EVA (A9918) uncross-linked			EVA (A9918) cross-linked			EVA (A9918) + catalyst cross-linked		
	Unexposed	Duplicates		Unexposed	Duplicates		Unexposed	Duplicates	
	# R213	# 212	# 221	# R45A	# 98	# 216	# RST2	# 64	# 16
0	0.243	0.183	0.216	0.246	0.210	0.195	0.249	0.258	0.294
0.506	0.269	0.208	0.219	0.258	0.237	0.209	0.256	0.257	0.263
2.862	0.308	0.237	0.254	0.275	0.252	0.223	0.258	0.280	0.292
5.3824	0.346	0.274	0.309	0.289	0.291	0.246	0.263	0.328	0.387
7.474	0.352	0.292	0.328	0.287	0.323	0.281	0.263	0.381	0.402
10.107	0.358	0.335	0.363	0.283	0.362	0.324	0.263	0.400	0.444
Slope m	0.0112	0.014	0.01151	0.0036	0.0141	0.012	0.0012	0.0154	0.0176
Correlation	0.93521	0.99235	0.99419	0.83493	0.99216	0.98504	0.85857	0.98529	0.95936

Table 15 (a, b, c) UV absorbance changes of (a) uncross-linked and (b) cross-linked EVA (Formula A9918) and (c) cross-linked EVA (Formula A9918 + Lupersol 101) films with outdoor exposure time

UV absorbance at 327 nm

Outdoor Exposure	Film Samples			Film Samples			Film Samples		
Toronto Summer Days	EVA (A9918) uncross-linked			EVA (A9918) cross-linked			EVA(A9918) + catalyst cross-linked		
	Unexposed	Duplicates		Unexposed	Duplicates		Unexposed	Duplicates	
	# R213	# 212	# 221	# R45A	# 98	# 216	# RST2	# 64	# 16
0	0.933	0.968	1.012	0.789	0.951	1.004	0.729	0.870	1.068
0.506	0.963	0.993	0.971	0.802	0.973	1.027	0.778	0.870	1.064
2.862	1.024	1.025	1.063	0.840	0.988	1.052	0.764	0.896	1.100
5.3824	1.087	1.066	1.123	0.894	1.050	1.078	0.778	0.944	1.219
7.474	1.096	1.078	1.131	0.839	1.055	1.105	0.755	1.002	1.210
10.107	1.102	1.114	1.171	0.863	1.085	1.139	0.760	1.008	1.244
Slope m	0.0171	0.0136	0.0197	0.0089	0.0131	0.0125	0.0008	0.016	0.0188
Correlation	0.93751	0.9867	0.95353	0.71684	0.97686	0.99372	0.17223	0.9732	0.95064

Table 16 (a, b, c) UV absorbance changes of (a) uncross-linked and (b) cross-linked EVA (Formula A9918) and (c) cross-linked EVA (Formula A9918 + Lupersol 101) films with outdoor exposure time

	UV absorbance at 287 nm								
Outdoor Exposure	Film Samples			Film Samples			Film Samples		
Toronto Summer Days	EVA (A9918) uncross-linked			EVA (A9918) cross-linked			EVA(A9918) + catalyst cross-linked		
	Unexposed	Duplicates		Unexposed	Duplicates		Unexposed	Duplicates	
	# R 213	# 212	# 221	# R45A	# 98	# 216	# RST2	# 64	# 16
0	1.329	1.380	1.440	1.092	1.392	1.500	1.050	1.254	1.545
0.506	1.356	1.420	1.447	1.105	1.439	1.535	1.122	1.269	1.526
2.862	1.440	1.473	1.512	1.167	1.475	1.597	1.098	1.316	1.599
5.3824	1.507	1.573	1.576	1.212	1.546	1.623	1.116	1.352	1.692
7.474	1.526	1.540	1.591	1.152	1.551	1.667	1.074	1.455	1.723
10.107	1.536	1.576	1.637	1.192	1.581	1.699	1.087	1.453	1.780
Slope m	0.0212	0.0181	0.0199	0.0089	0.0177	0.0187	0	0.0213	0.0266
Correlation	0.94793	0.97842	0.98702	0.75126	0.95935	0.98035	-0.00308	0.97006	0.9888

Table 17 (a, b, c) Changes of UV absorbance of (a) uncross-linked and (b) cross-linked EVA (Formula A9918) and (c) cross-linked EVA (Formula A9918 + Lupersol 101) films with outdoor exposure time

	UV absorbance difference at 210-220 nm					
Outdoor Exposure	Film Samples		Film Samples		Film Samples	
Toronto Summer Days	EVA (A9918) uncross-linked Duplicates		EVA (A9918) cross-linked Duplicates		EVA(9918) + catalyst cross-linked Duplicates	
	# 212/R213	# 221/R213	# 98/R45A	# 216/R45A	# 64/RST2	# 16/RST2
0	0.3039	0.4095	0.4095	0.2412	0.393	0.5316
0.506	0.1406	0.1653	0.4685	0.5366	0.3518	0.5811
2.862	0.1059	0.1257	0.3567	0.492	0.3435	0.6603
5.3824	0.1257	0.195	0.4095	0.4656	0.4392	0.7758
7.474	0.03	0.0861	0.413	0.4857	0.455	0.8154
10.107	0.1026	0.2049	0.4706	0.525	0.459	0.871
Slope m	-0.0155	-0.0135	0.0026	0.0134	0.0106	0.0334
Correlation	-0.67885	-0.50042	0.24714	0.49033	0.82425	0.98425

Table 18 (a, b) IR absorbance of (a) uncross-linked and (b) cross-linked ELVAX 150 films at 3100 cm^{-1} following irradiation in accelerated ager

Irradiation Time Toronto Summer Days	IR absorbance at 3100 cm^{-1} Film Samples ELVAX 150 uncross-linked Duplicates # 54	# 59	Film Samples ELVAX 150 cross-linked Duplicates # 58A	# 40
0	0.0269	-0.0212	-0.0034	-0.0007
10.48	0.0061	0.0144	0.0032	0.0082
19.243	-0.011	-0.0113	0.0183	0.0293
29.938	0.0007	0.0236	0.0426	0.0411
38.428	0.0149	0.0306	0.0605	0.0535
47.699	0.0209	0.0499	0.0802	0.0924
58.002	0.0447	0.063	0.0969	0.0716
66.789	0.0633	0.0779	0.1189	0.127
75.618	0.0757	0.0936	0.1227	0.1288
85.116	0.0792	0.0985	0.1558	0.1399
91.844	0.0987	0.1254	0.2234	0.149
99.891	0.1177	0.1423	0.2273	0.2162
105.38	0.1249	0.1684	0.2553 (failed)	0.2685
115.048	0.1411	0.2041	-	0.1861
123.595	0.123	-	-	0.2443
132.621	0.2285	0.2012	-	0.3066
142.891	-	-	-	-
Slope m correlation	0.0017 0.95743	0.0019 0.98485	0.0024 0.97468	0.0022 0.95857

Table 18c Changes of IR absorbance at 3100 cm^{-1} of low density Polyethylene following irradiation in accelerated ager

Irradiation Time Toronto Summer Days	IR absorbance at 3100 cm^{-1} Film Samples Polyethylene (low density) # 303	# 304
0	0.0086	0.0043
10.48	0.0128	0.0128
19.243	0.0212	0.0212
29.938	0.017	0.0253
38.428	0.017	0.0334
47.699	0.0531	0.0531
58.002	0.0607	0.0682
66.769	0.0645	0.0682
75.618	0.0828	0.1004
85.116	0.1106	0.0792
91.844	0.1335	0.1173
99.891	0.1523	0.1553
105.38	0.143	0.135 (broken)
115.048	0.179	-
123.595	0.2041	-
132.621	0.2672	-
142.891	-	-
Slope m correlation	0.0018 0.95409	0.0013 0.95957

Table 19 % Gel content for various films after outdoor or accelerated ager exposure

Films	Weather-O-meter Irradiation Time (Toronto Summer Days)	% Gel Content
ELVAX 150	0	1.19
	10.243	2.9
	29.938	0.7
	38.428	0.15
	58.002	0.91
	75.618	0.94
	85.116	1.47
	115.048	1.57
ELVAX 150 cross-linked	0	93.17 and 14.47
EVA (Formula A9918)		
uncross-linked	0	2.65
cross-linked	0	77.48
	19.243	59.78
	29.938	86.48
	38.428	71.40
	58.002	83.48
	75.618	70.13
	85.116	91.49
	115.048	90.36
Low Density Polyethylene	0	66.67
	142.874	70.77
	Outdoor Weathering (Toronto Summer Days)	
EVA (Formula A9918) cross-linked	0.504	78.10
	2.862	82.35
	5.3824	84.48
	7.474	78.08
	10.107	80.00

Table 20 Elemental analysis of unexposed and irradiated EVA films

Films	C	H	O	Average O Content
ELVAX 150 uncross-linked, unexposed	76.43	12.51	11.06	11.09%
	73.34	12.54	11.12	
ELVAX 150 uncross-linked at point of failure	72.13	11.39	16.48	16.46%
	72.29	11.27	16.44	
ELVAX 150 cross-linked, unexposed	76.00	12.56	11.49	11.505%
	75.97	12.51	11.52	
at point of failure	69.50	10.80	19.7	19.60%
	69.62	10.88	19.5	
ELVAX (Formula A9918) uncross-linked, unexposed	76.50	12.61	10.89	11.02%
	76.29	12.56	11.15	
at 142.874 Toronto Summer Days	76.46	12.74	10.80	10.995%
	76.22	12.59	11.19	
cross-linked, unexposed	75.72	12.45	11.85	11.62%
	75.98	12.61	11.41	
at 142.874 Toronto Summer Days	75.94	12.48	11.58	11.62%
	76.11	12.37	11.52	
Low Density Polyethylene unexposed	84.84	15.13	0.03	0.13%
	84.75	15.02	0.23	
at point of brittleness	81.69	13.82	4.49	4.48%
	81.62	13.91	4.47	

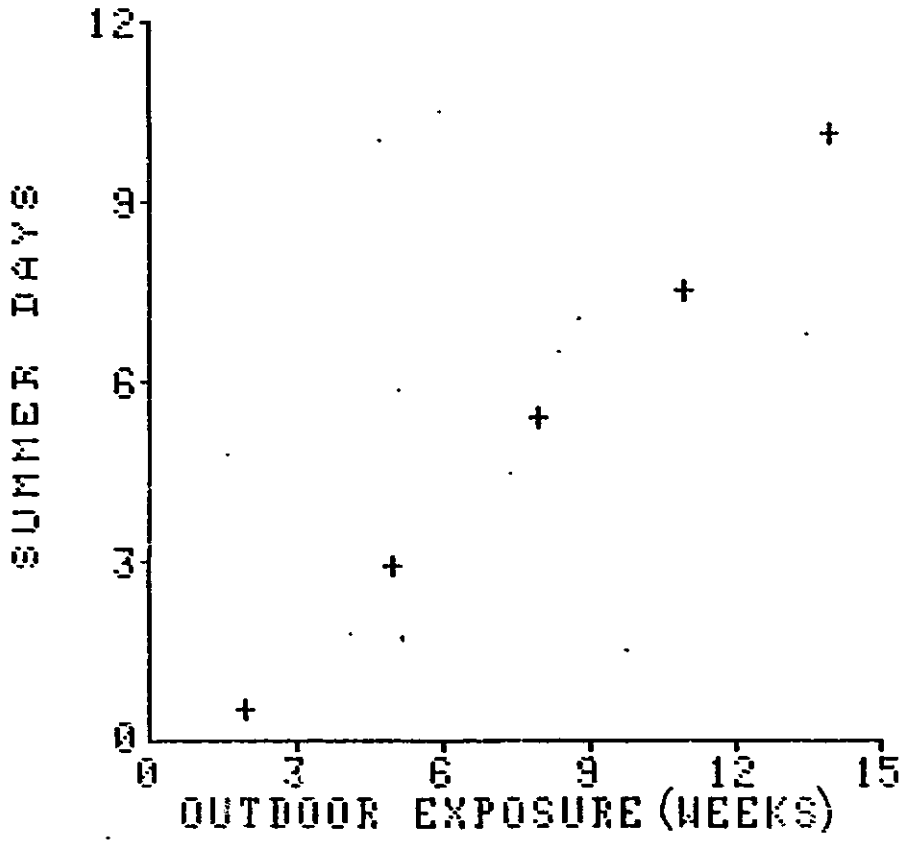

Fig. 1. Equivalent solar exposure (summer days) vs. actual outdoor exposure time (Nov. 15, 1983 - Feb. 24, 1984)

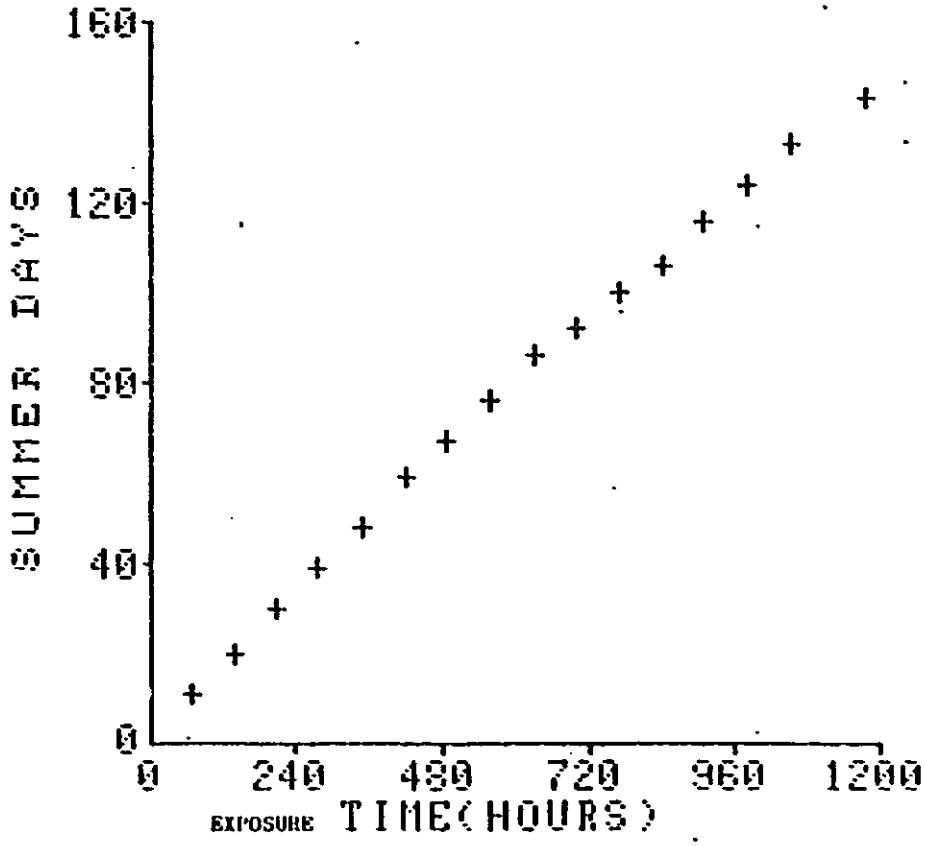

Fig. 2. Equivalent solar exposure (summer days) vs. actual accelerated ager exposure time.

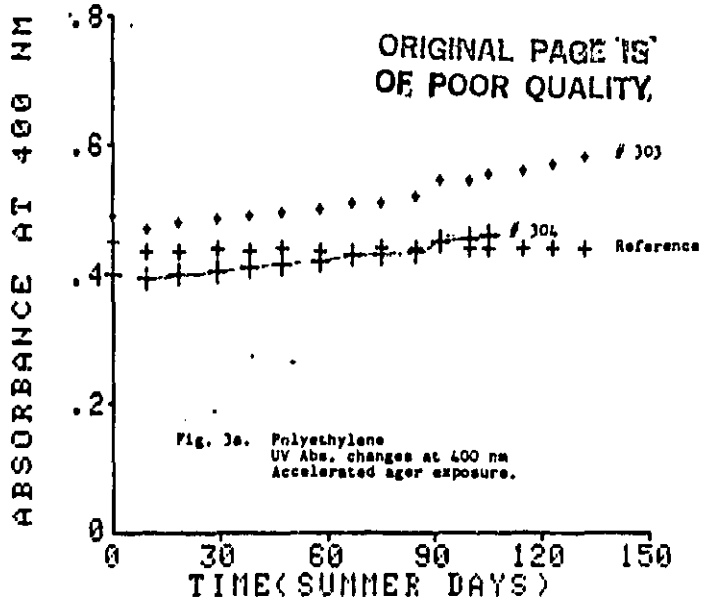

Fig. 3a. Polyethylene
UV Abs. changes at 400 nm
Accelerated ager exposure.

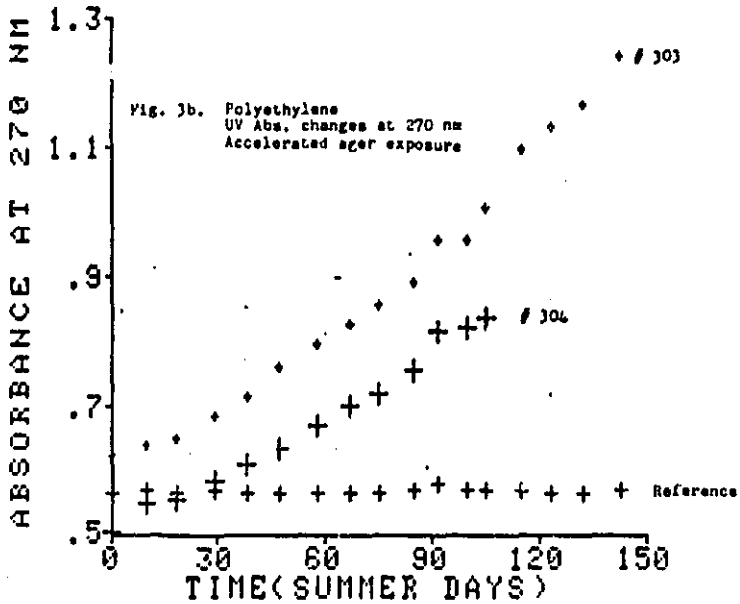

Fig. 3b. Polyethylene
UV Abs. changes at 270 nm
Accelerated ager exposure

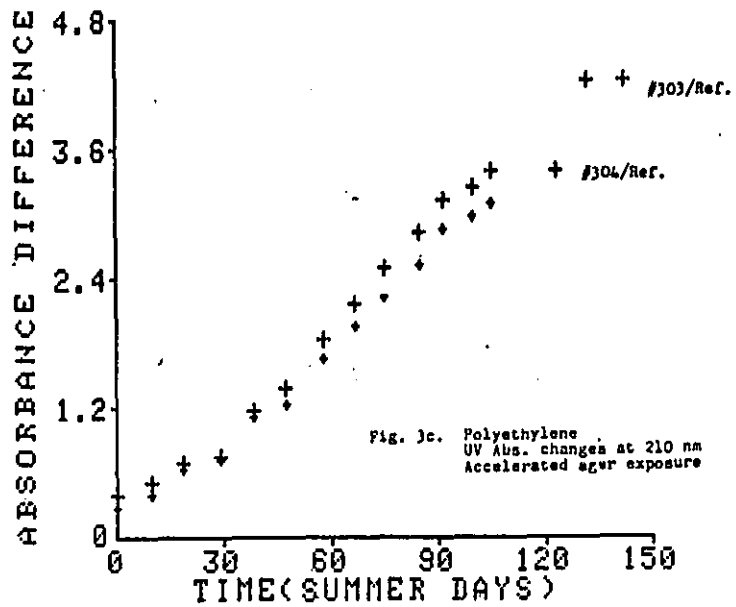

Fig. 3c. Polyethylene
UV Abs. changes at 210 nm
Accelerated ager exposure

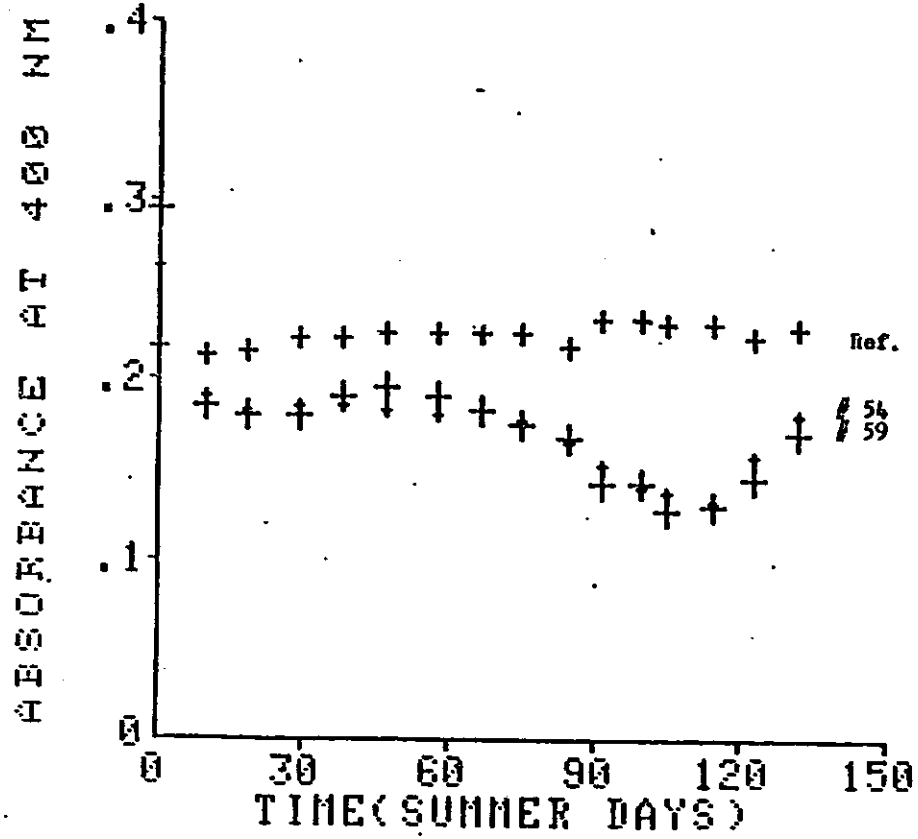

Fig. 4a. Elvax 150, uncrosslinked UV Abs. changes at 400 nm Accelerated ager exposure.

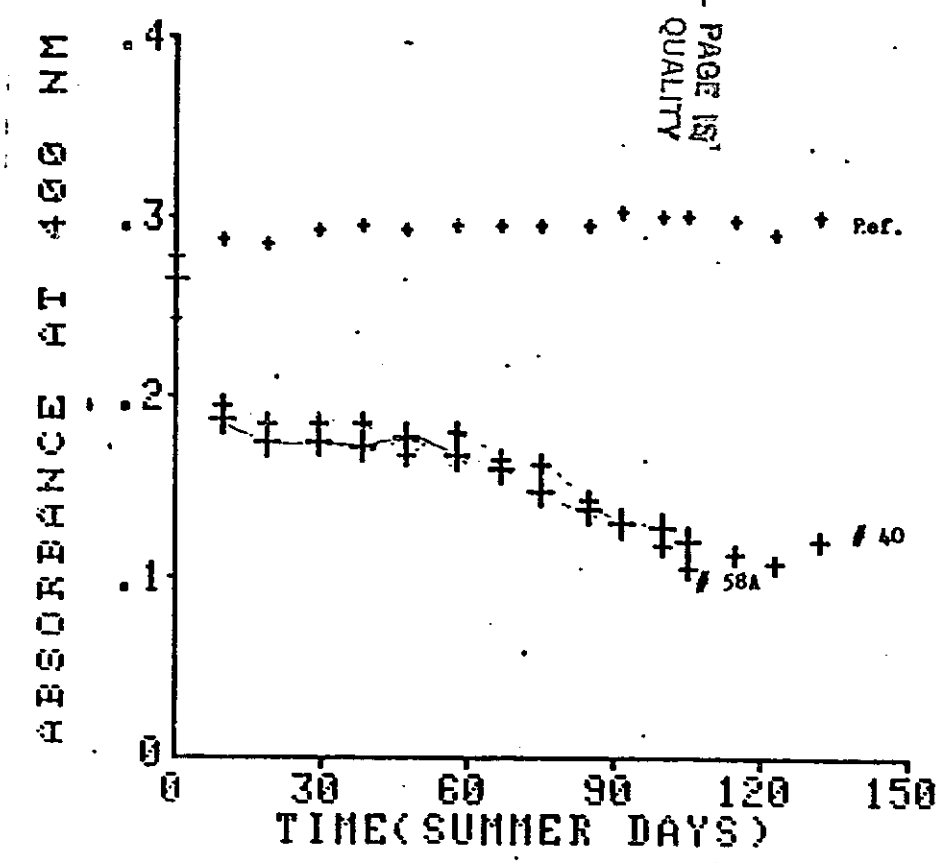

Fig. 4b. Elvax 150, crosslinked UV Abs. changes at 400 nm Accelerated ager exposure.

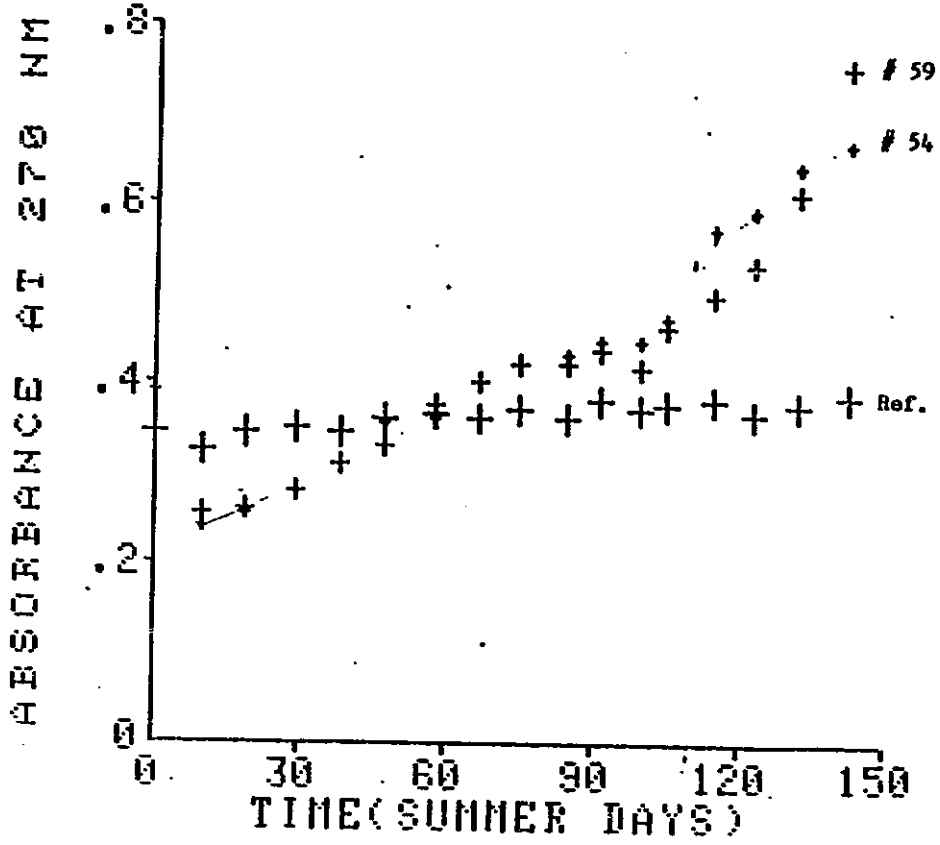

Fig. 5a. Elvax 150, uncrosslinked UV Abs. changes at 270 nm Accelerated ager exposure.

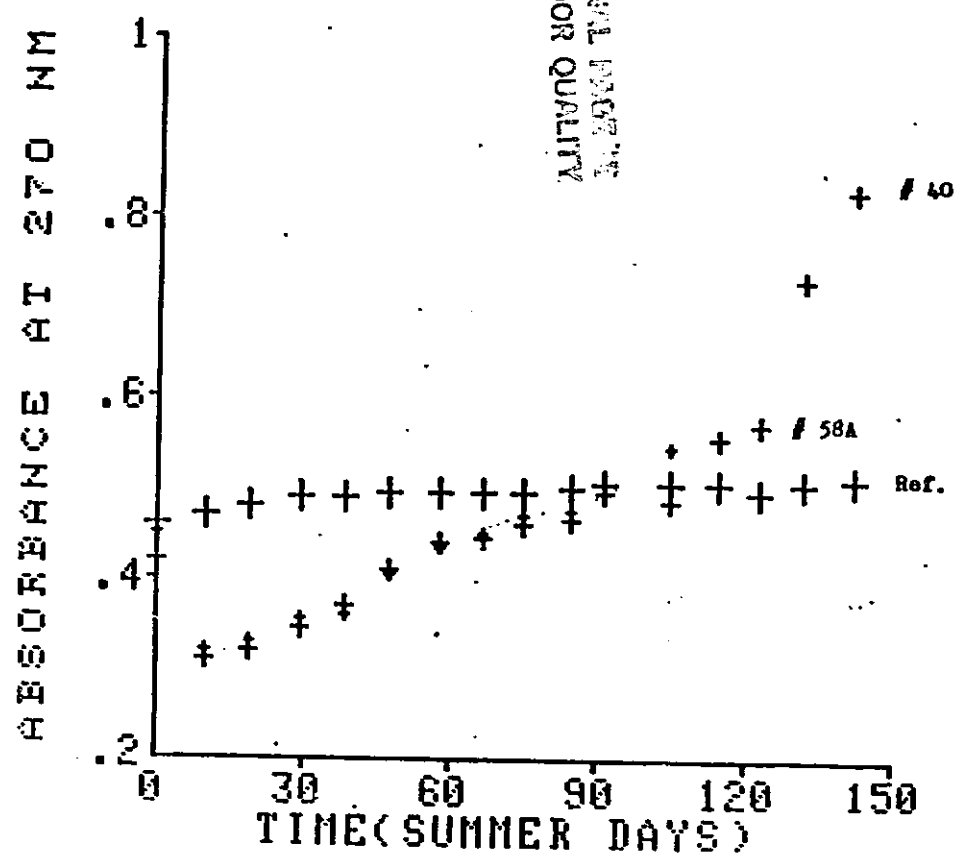

Fig. 5b. Elvax 150, crosslinked UV Abs. changes at 270 nm Accelerated ager exposure.

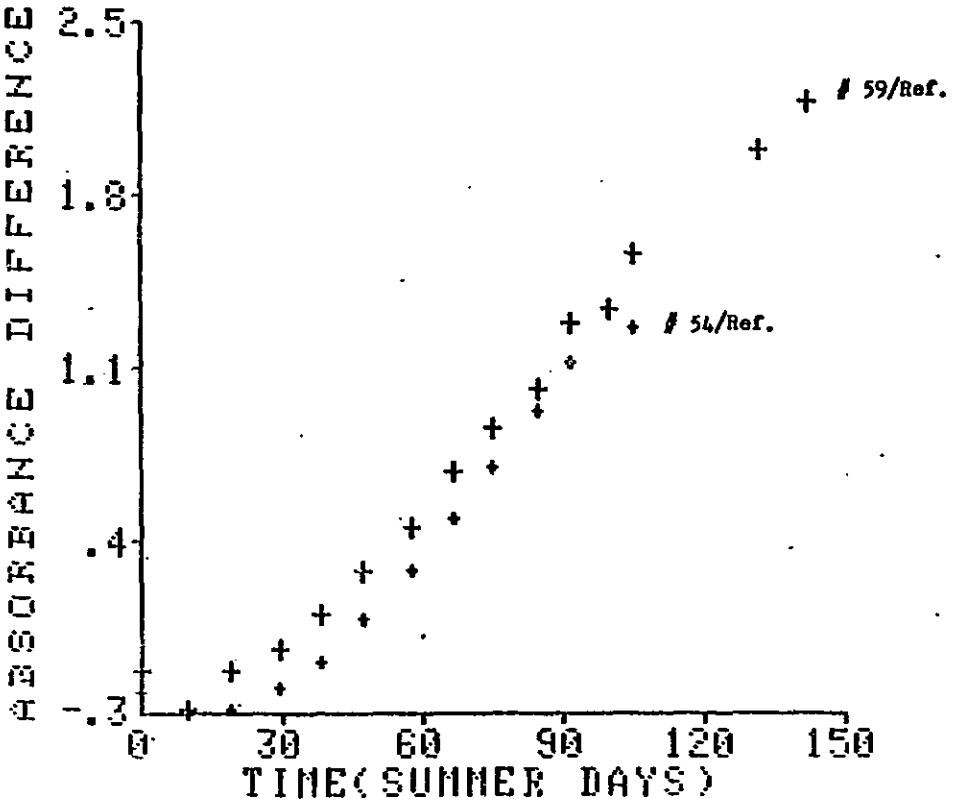

Fig. 6a. Elvax 150, uncrosslinked UV Abs. changes at 215 nm Accelerated ager exposure.

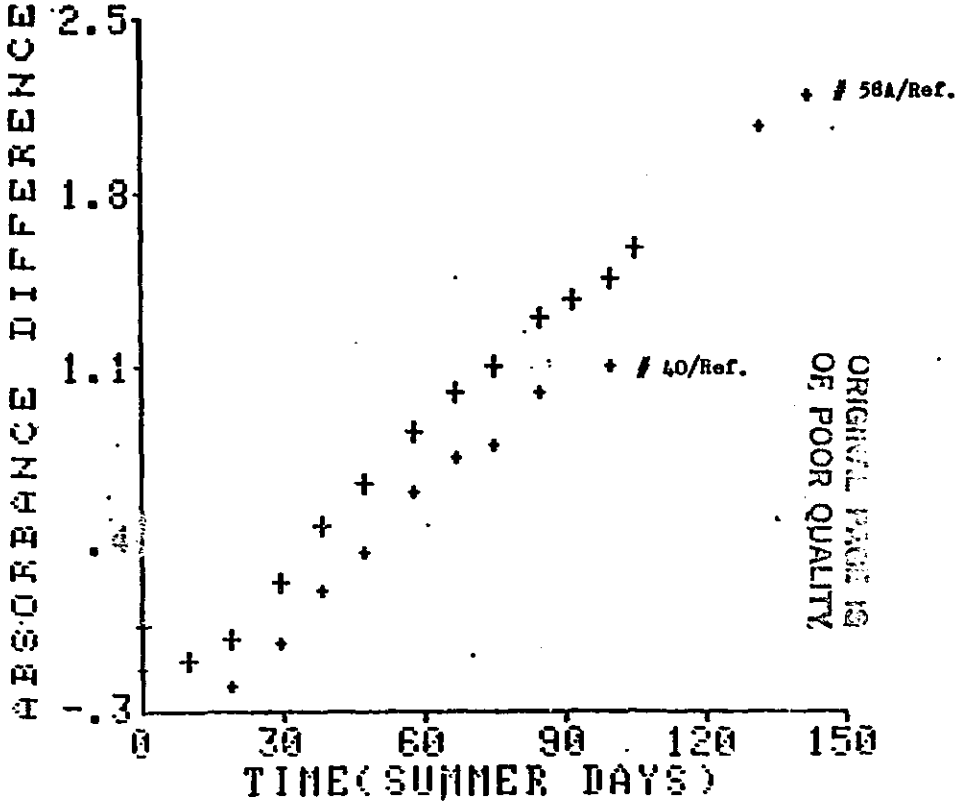

Fig. 6b. Elvax 150, crosslinked UV Abs. changes at 215 nm Accelerated ager exposure.

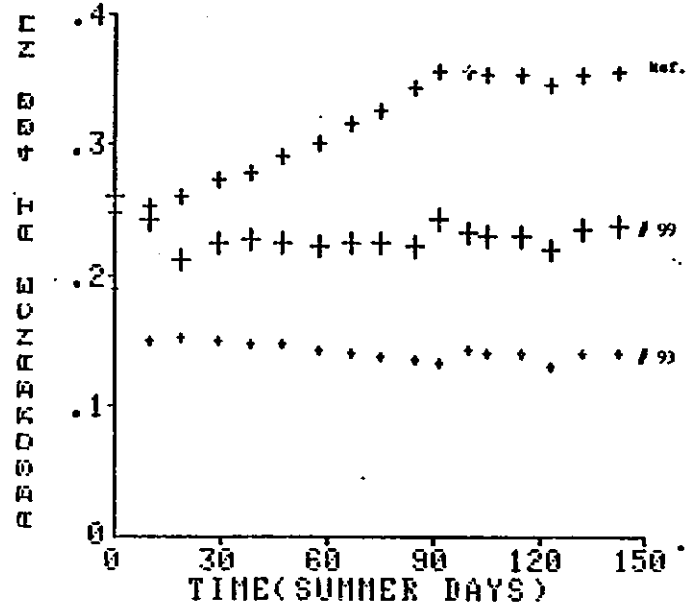

Fig. 7a. A9918, uncrosslinked UV Abs. changes at 400 nm Accelerated ager exposure.

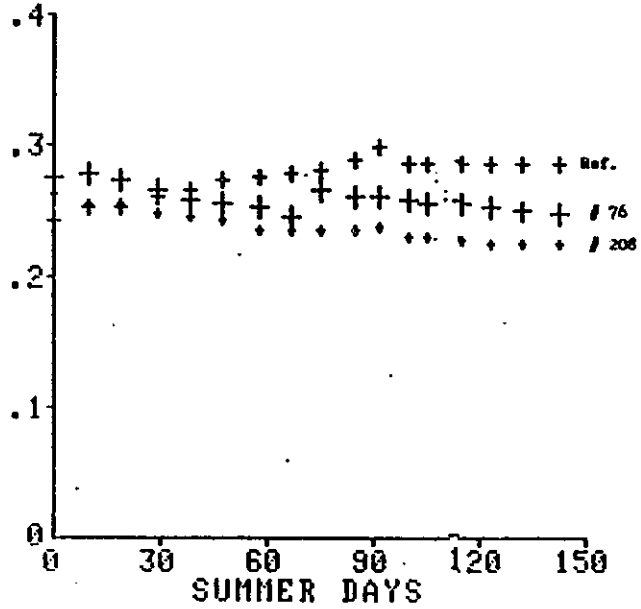

Fig. 7b. A9918, crosslinked UV Abs. changes at 400 nm Accelerated ager exposure.

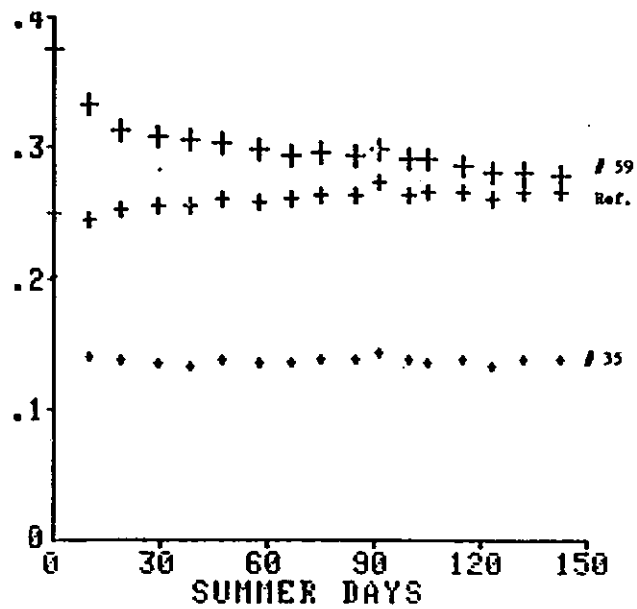

Fig. 7c. A9918 + Lupersol 101, crosslinked UV Abs. changes at 400 nm Accelerated ager exposure.

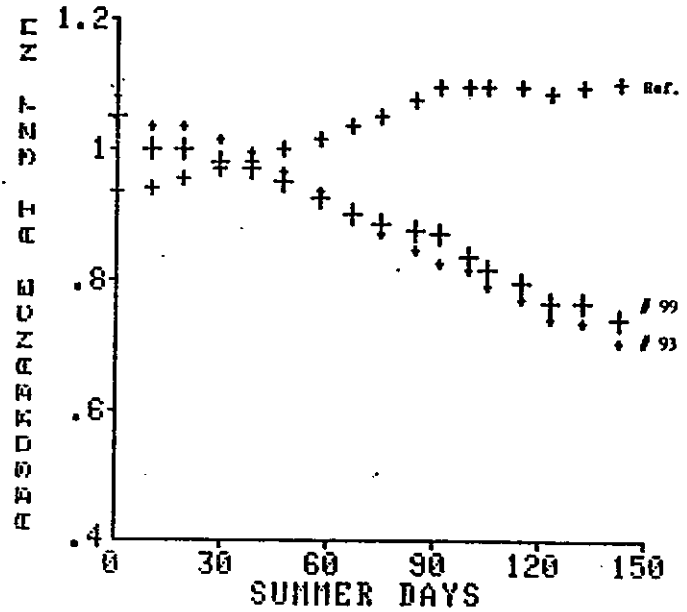

Fig. 8a. A9918, uncrosslinked UV Abs. changes at 327 nm Accelerated ager exposure.

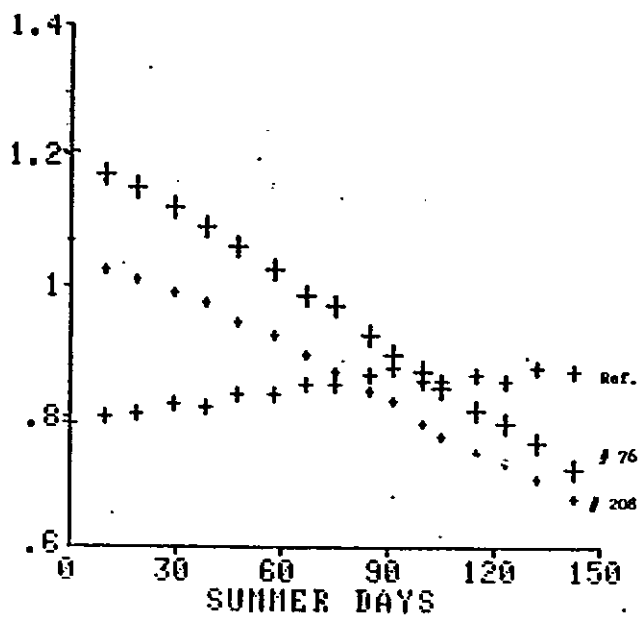

Fig. 8b. A9918, crosslinked UV Abs. changes at 327 nm Accelerated ager exposure.

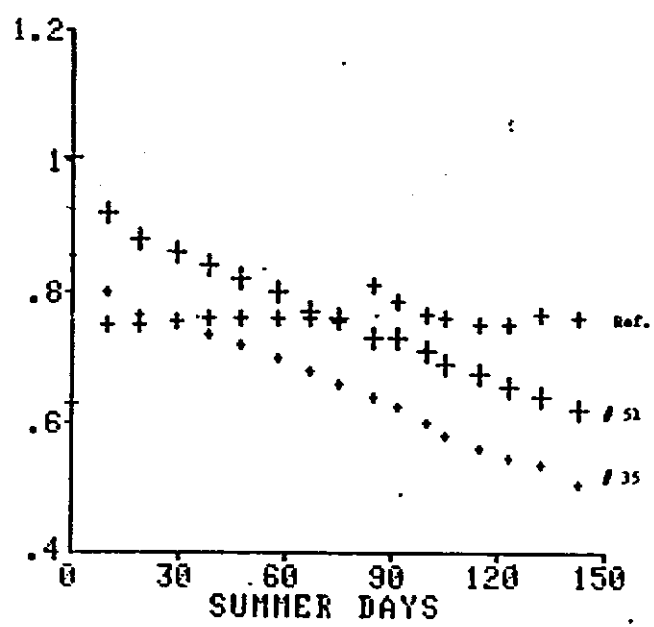

Fig. 8c. A9918 + Lupersol 101, crosslinked UV Abs. changes at 327 nm Accelerated ager exposure.

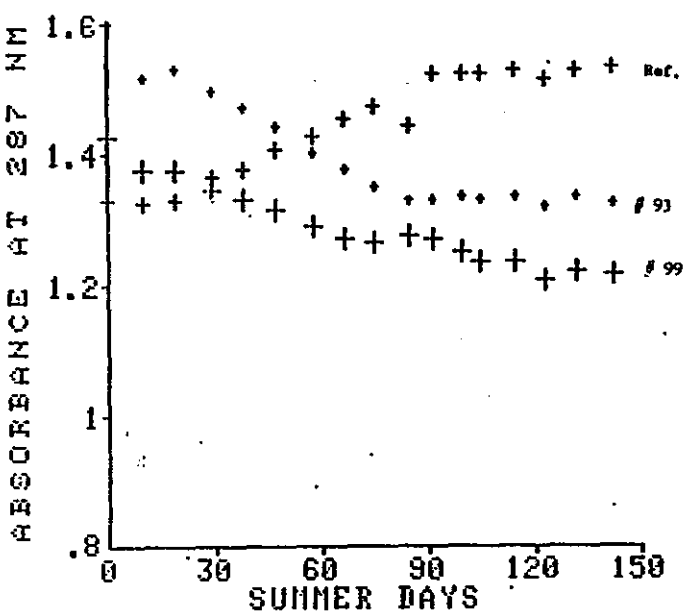

Fig. 9a. A9918, uncrosslinked UV Abs. changes at 287 nm Accelerated ager exposure.

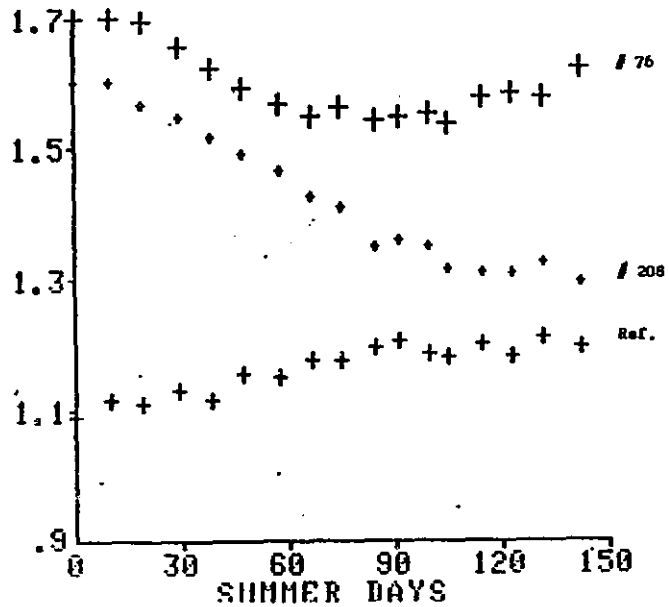

Fig. 9b. A9918, crosslinked UV Abs. changes at 287 nm Accelerated ager exposure.

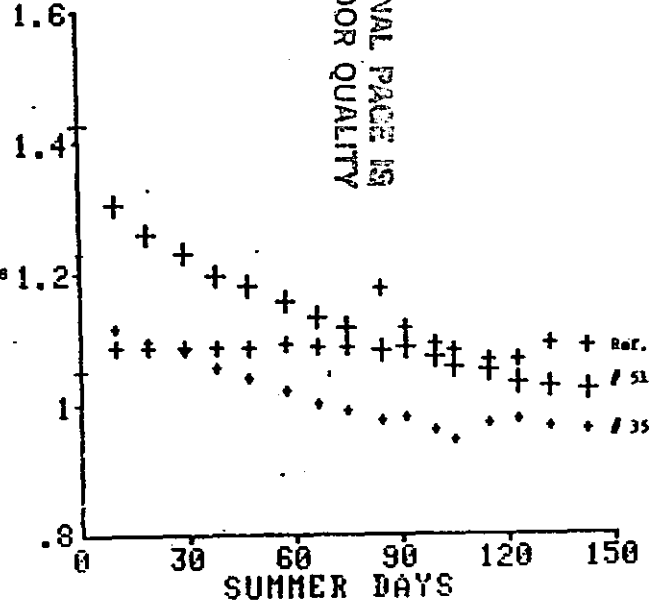

Fig. 9c. A9918 + Lupersol 101, crosslinked UV Abs. changes at 287 nm Accelerated ager exposure.

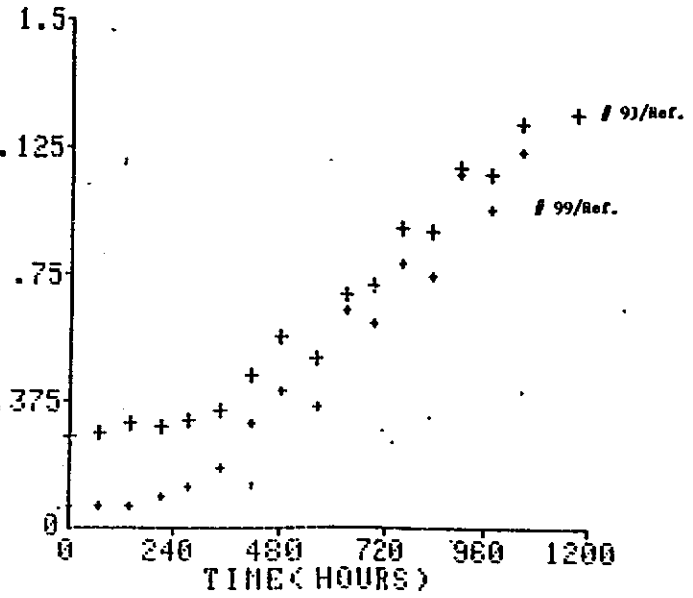

Fig. 10a. A9918, uncrosslinked UV Abs. changes at 215 nm (relative to unexposed sample). Accelerated ager exposure.

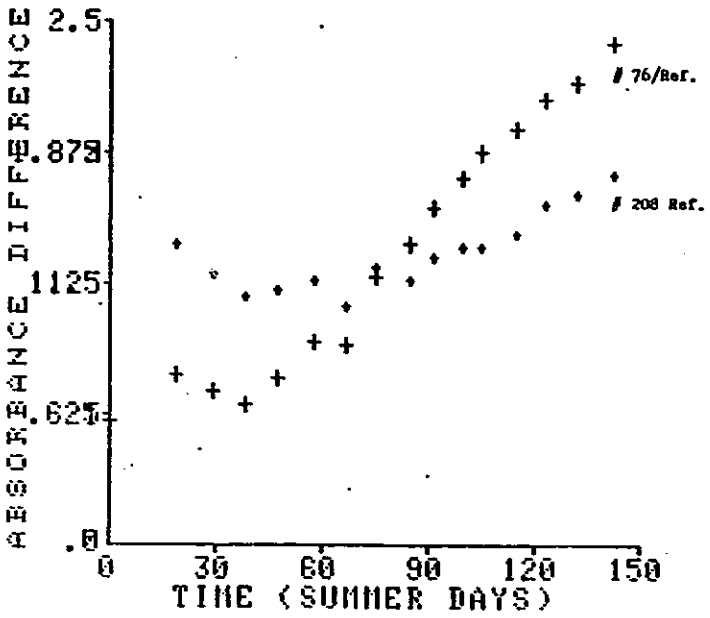

Fig. 10b. A9918, crosslinked UV Abs. changes at 215 nm (relative to unexposed sample) Accelerated ager exposure.

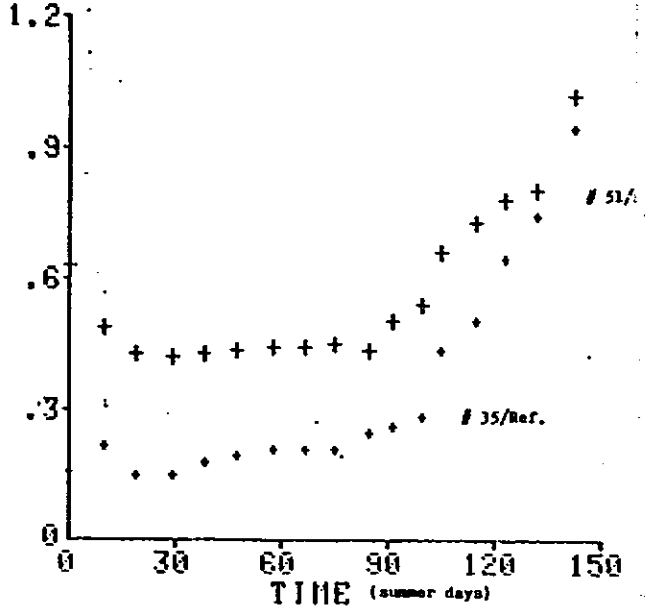

Fig. 10c. A9918 + Lupersol 101, crosslinked UV Abs. changes (relative to unexposed sample) Accelerated ager exposure.

215 nm

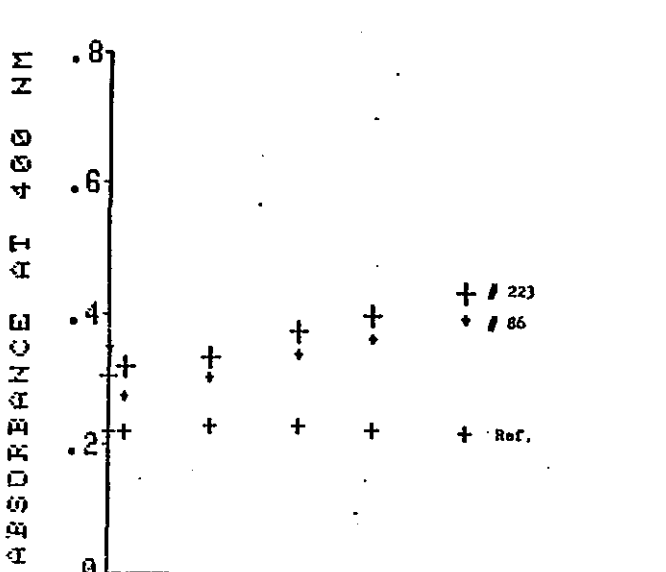

Fig. 11a. Elvax 150, uncrosslinked UV Abs. changes at 400 nm Outdoor exposure.

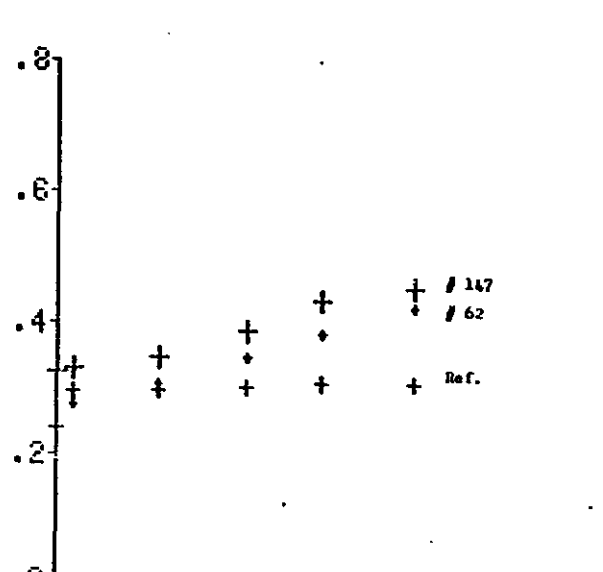

Fig. 11b. Elvax 150, crosslinked UV Abs. changes at 400 nm Outdoor exposure.

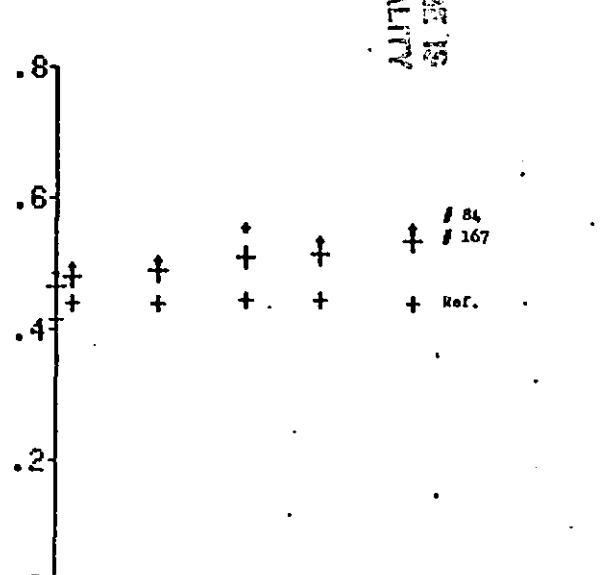

Fig. 11c. Polyethylene
UV Abs. changes at 400 nm
Outdoor exposure.

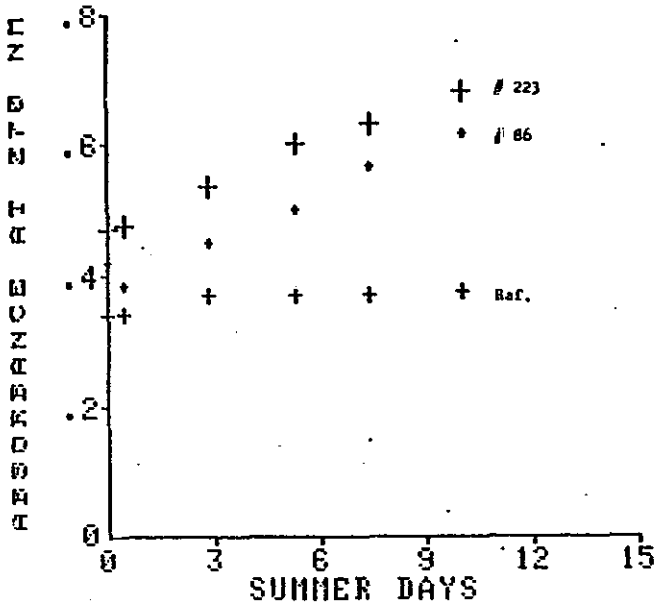

Fig. 12a. Elvax 150, uncrosslinked UV Abs. changes at 270 nm Outdoor exposure.

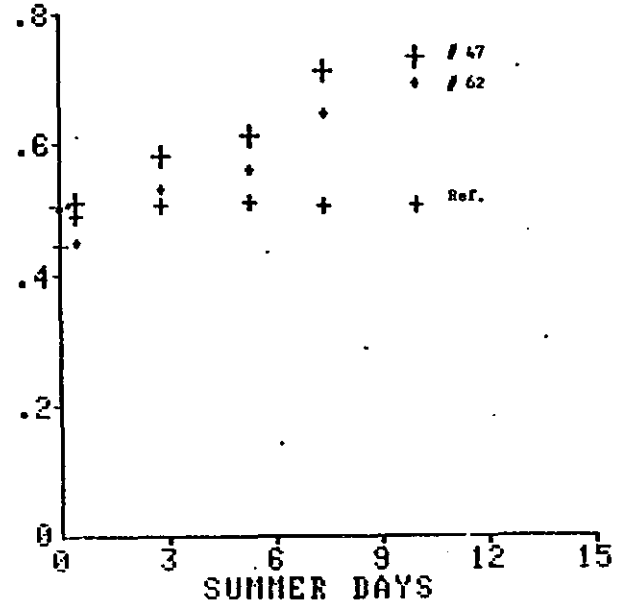

Fig. 12b. Elvax 150, crosslinked UV Abs. changes at 270 nm Outdoor exposure.

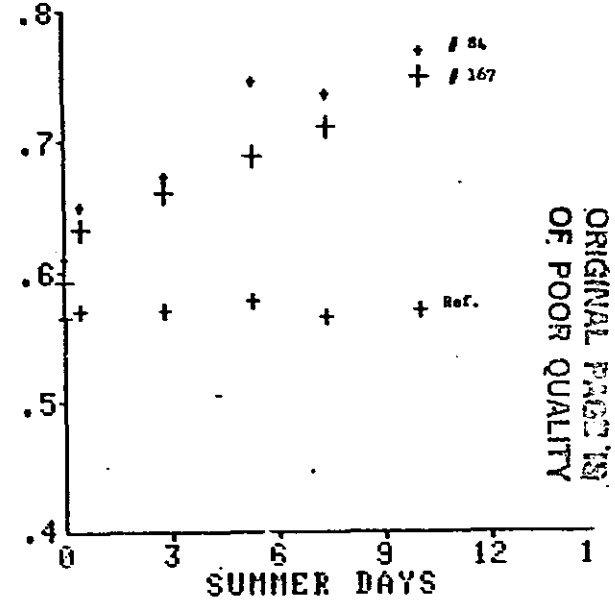

Fig. 12c. Polyethylene.
UV Abs. changes at 270 nm
Outdoor exposure.

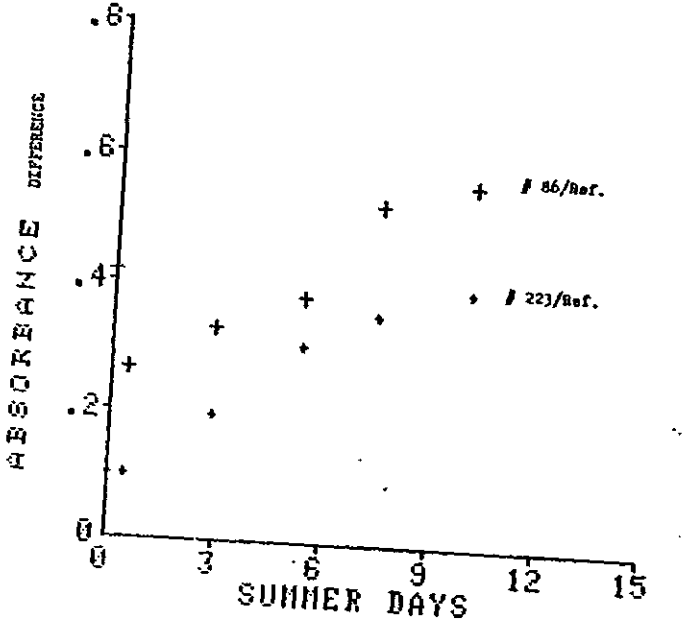

Fig. 13a. Elvax 150, uncrosslinked UV Abs. changes at 215 nm Outdoor exposure.

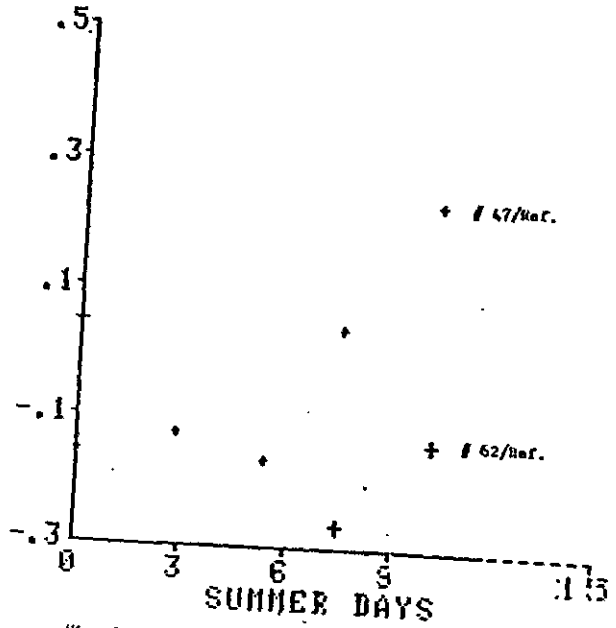

Fig. 13b. Elvax 150, crosslinked UV Abs. changes at 215 nm. Outdoor exposure.

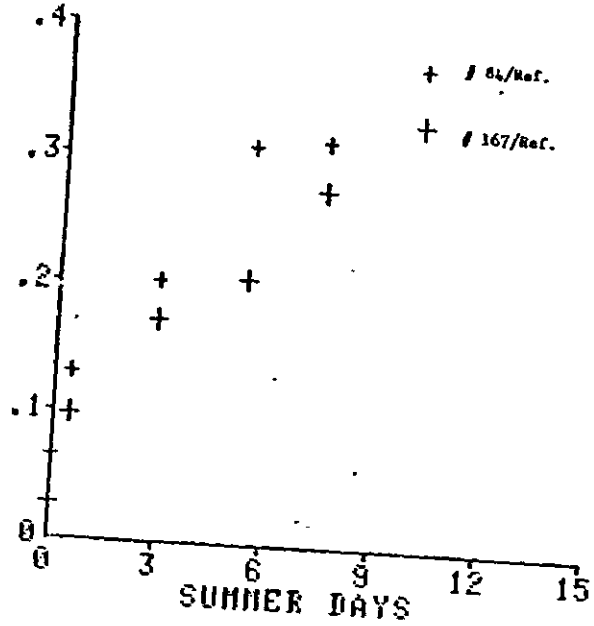

Fig. 13c. Polyethylene UV Abs. changes at 210 nm. Outdoor exposure.

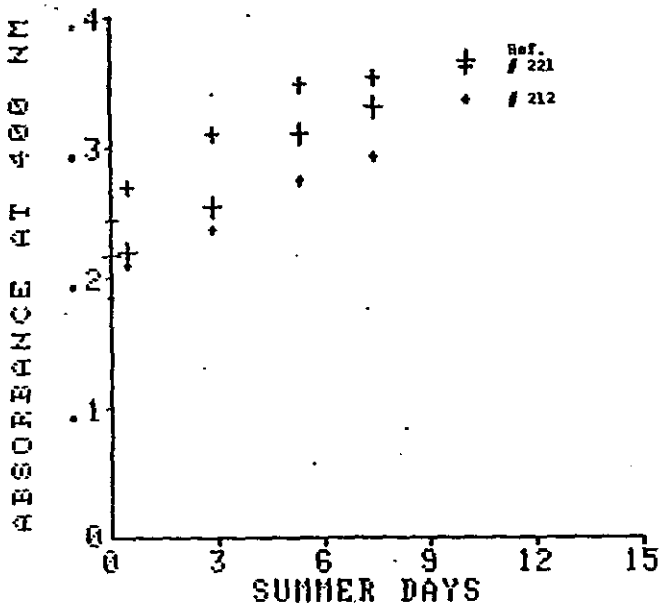

Fig. 14a. A9918, uncrosslinked UV Abs. changes at 400 nm. Outdoor exposure.

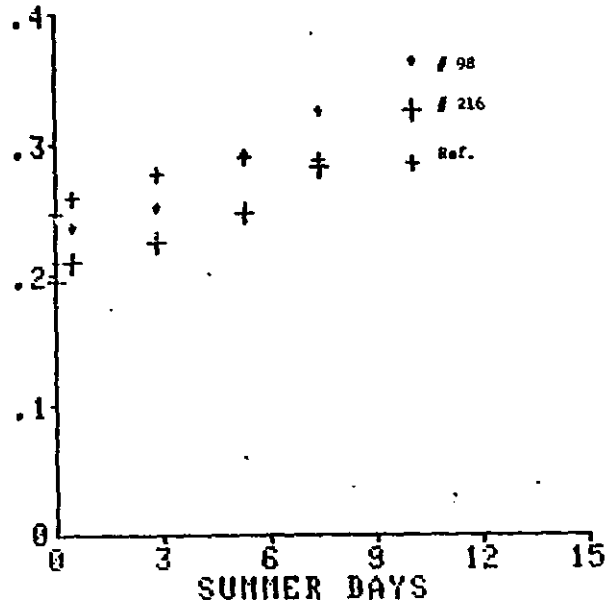

Fig. 14b. A9918, crosslinked UV Abs. changes at 400 nm. Outdoor exposure.

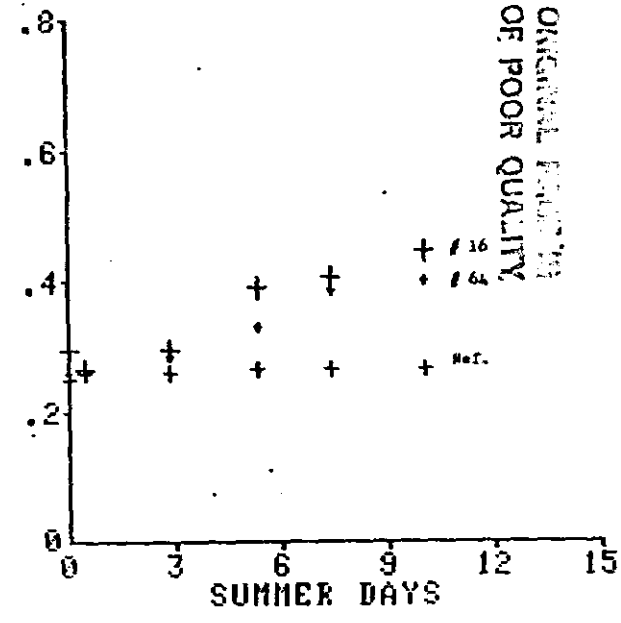

Fig. 14c. A9918 + Lupersol 101, crosslinked UV Abs. changes at 400nm. Outdoor exposure.

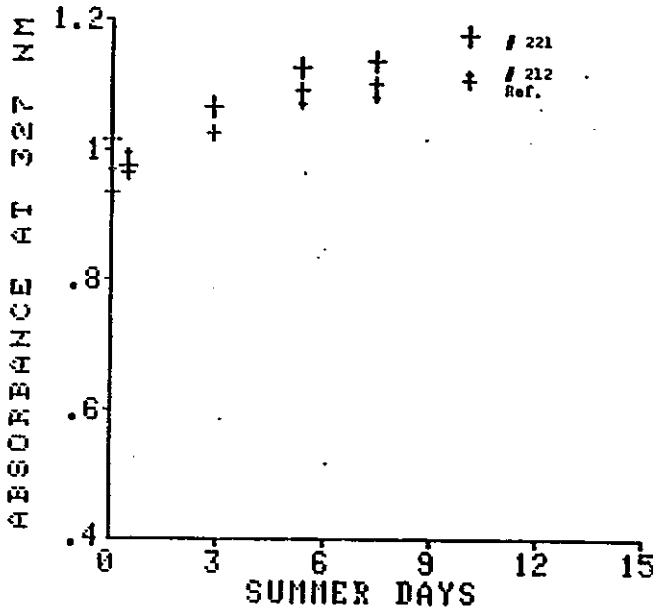

Fig. 15a. A9918, uncrosslinked UV Abs. changes at 327 nm. Outdoor exposure.

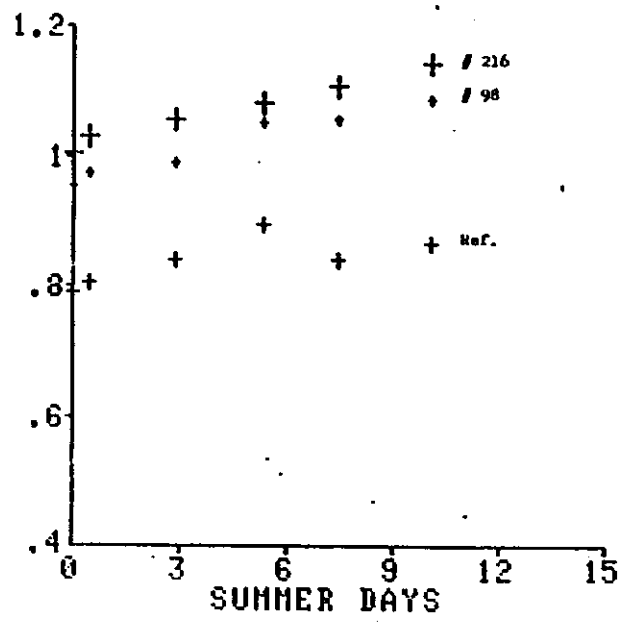

Fig. 15b. A9918, crosslinked UV Abs. changes at 327 nm. Outdoor exposure.

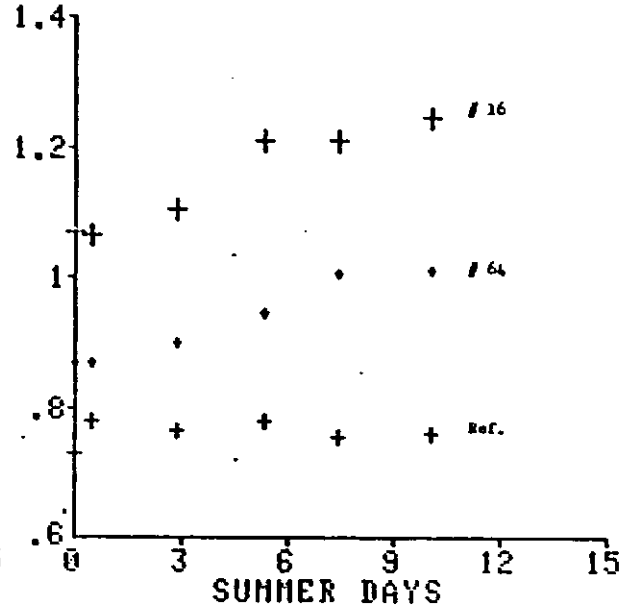

Fig. 15c. A9918 + Lupersol 101, crosslinked UV Abs. changes at 327 nm. Outdoor exposure.

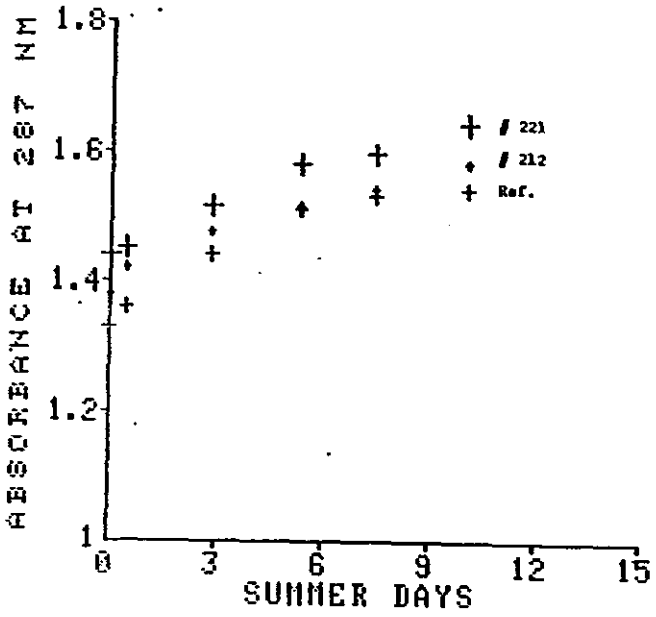

Fig. 16a. A9918, uncrosslinked UV Abs. changes at 287 nm. Outdoor exposure.

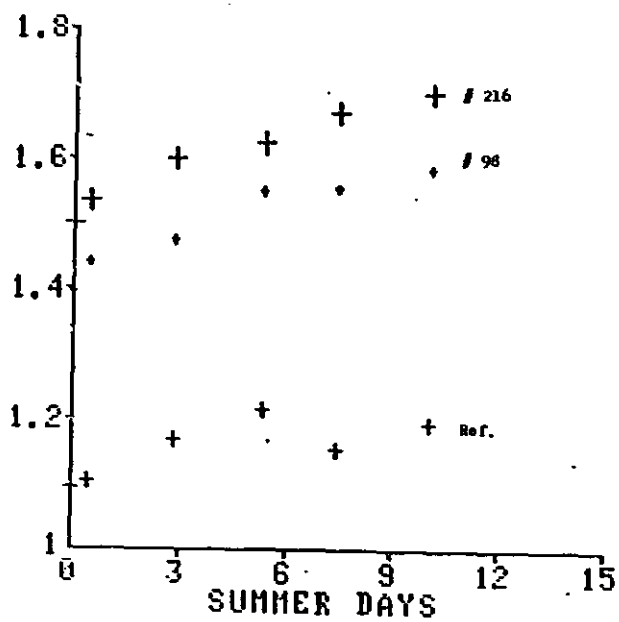

Fig. 16b. A9918, uncrosslinked UV Abs. changes at 287 nm. Outdoor exposure.

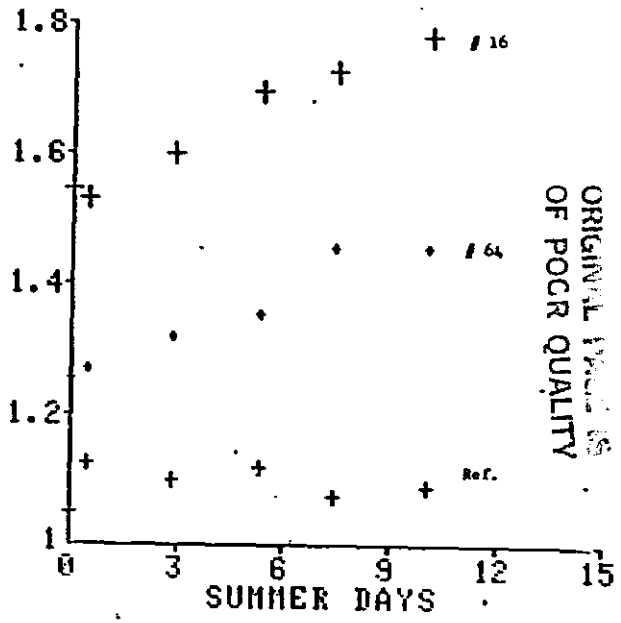

Fig. 16c. A9918 + Lupersol 101, crosslinked UV Abs. changes at 287 nm.
Outdoor exposure.

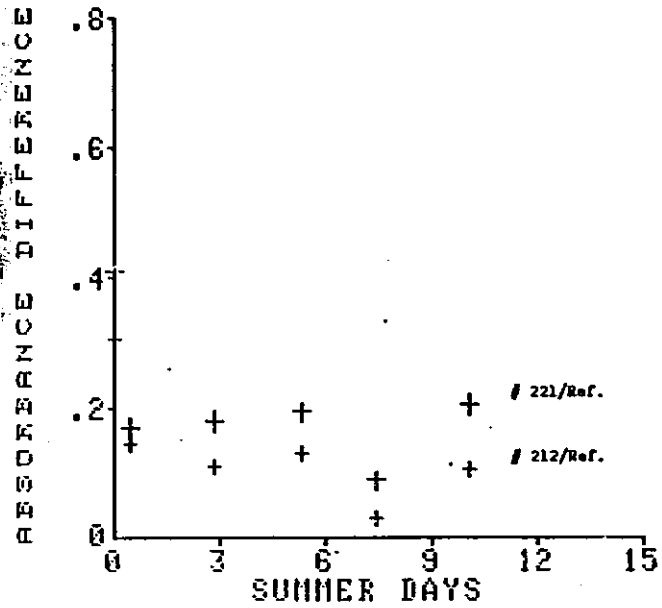

Fig. 17a. A9918, uncrosslinked UV Abs. changes at 215 nm. Outdoor exposure.

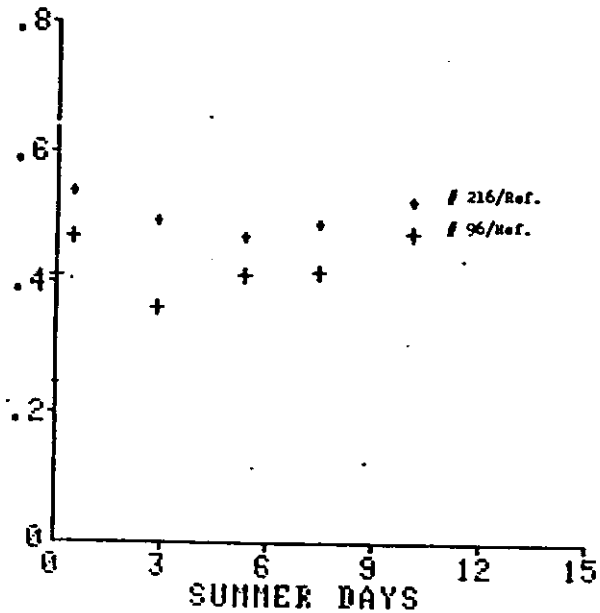

Fig. 17b. A9918, crosslinked UV Abs. changes at 215 nm. Outdoor exposure.

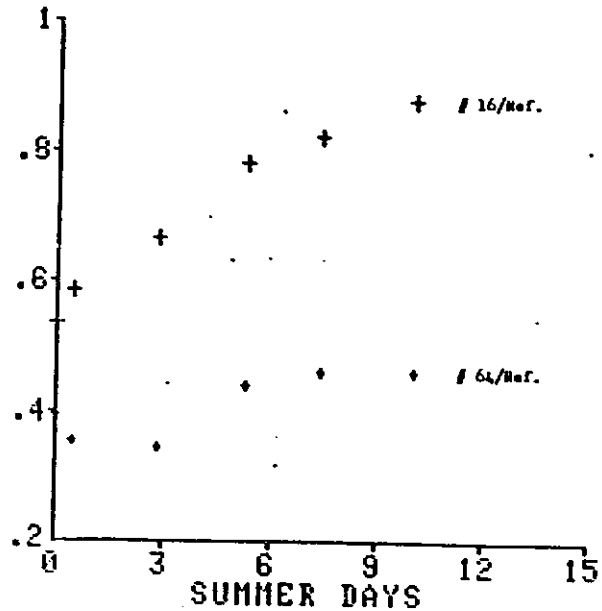

Fig. 17c. A9918 + Lupersol 101, crosslinked UV Abs. changes at 215 nm. Outdoor exposure.

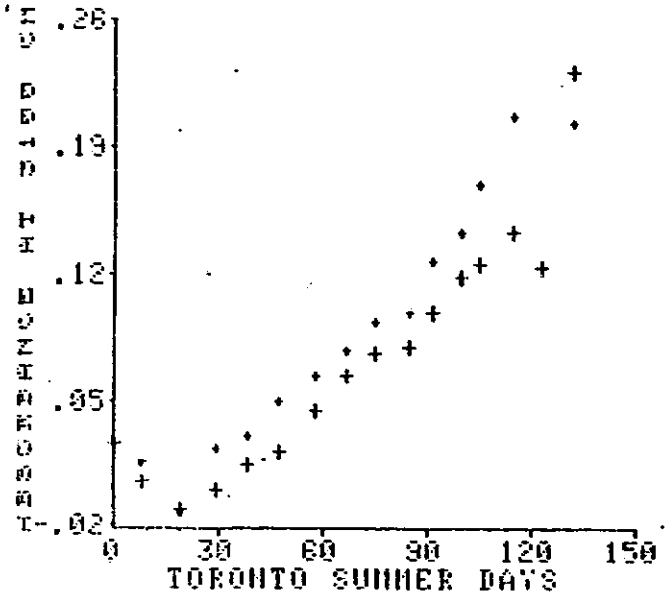

Fig. 18a. Elvax 150, uncrosslinked IR Abs. changes at 3100 cm^{-1} Accelerated ager exposure.

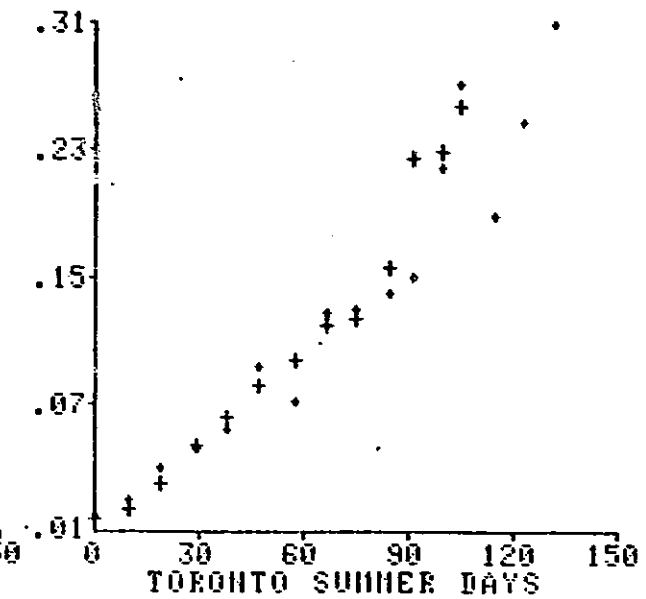

Fig. 18b. Elvax 150, uncrosslinked IR Abs. changes at 3100 cm^{-1}. Accelerated ager exposure.

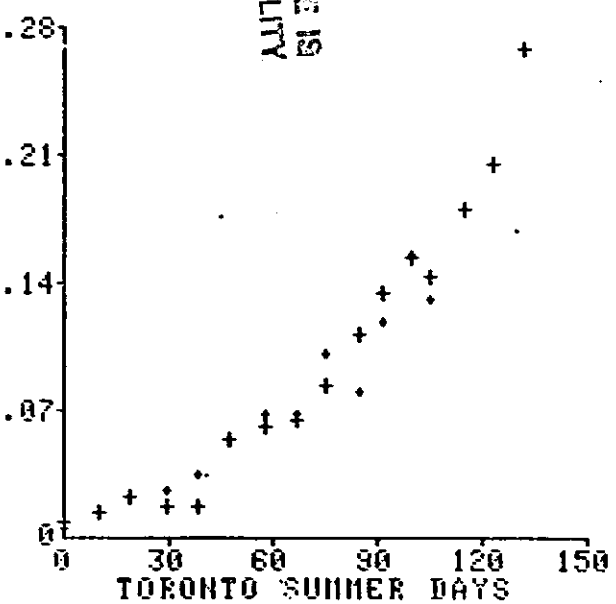

Fig. 18c. Polyethylene. IR Abs. changes at 3100 cm^{-1}. Accelerated ager exposure.

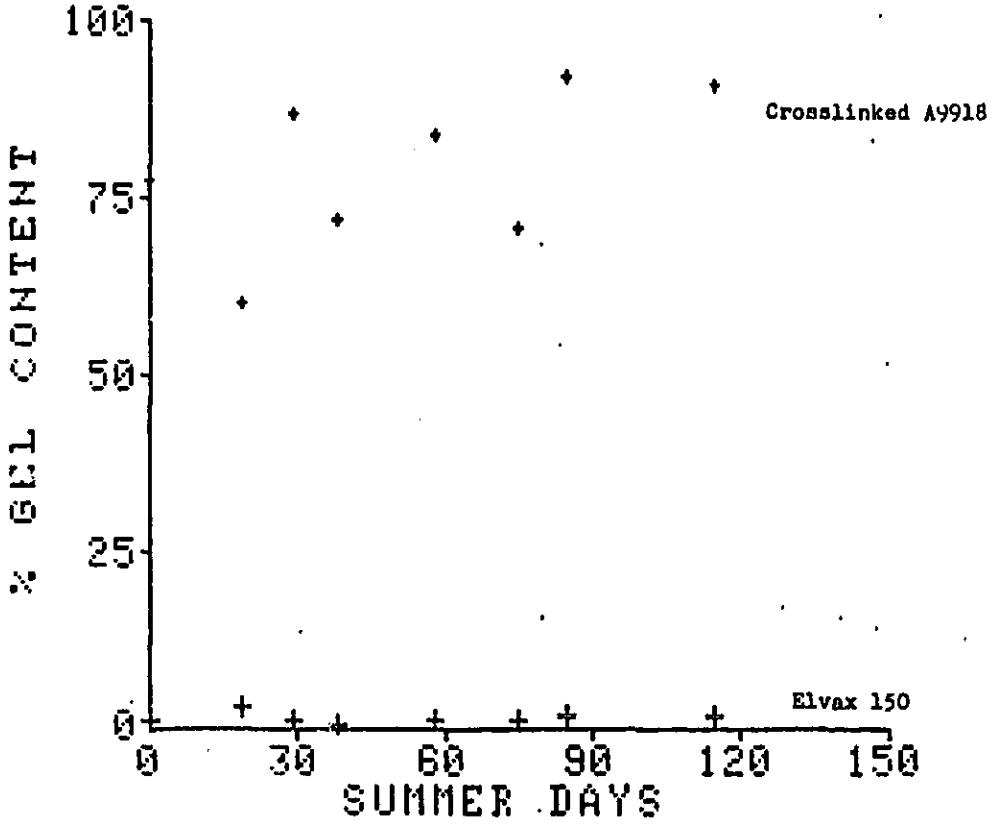

Fig. 19. % gel content of Elvax 150 and crosslinked A9918 vs. accelerated ager exposure level.

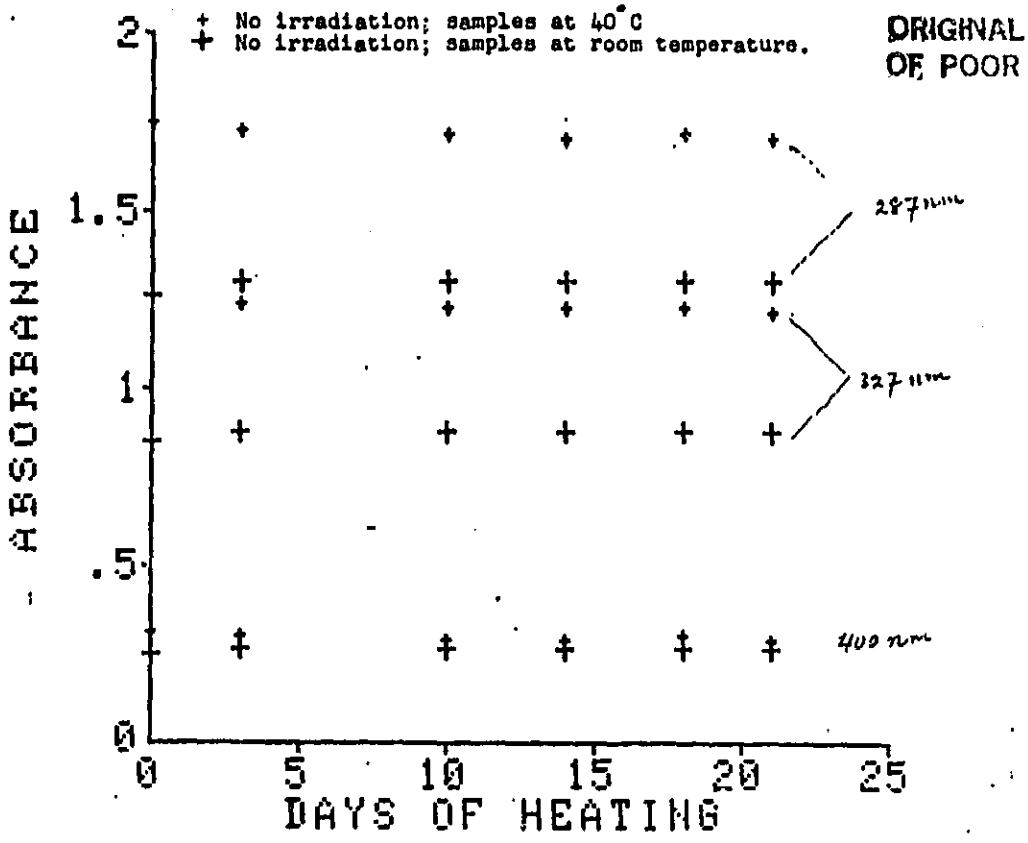

Fig. A1. A9918, crosslinked, UV Abs. changes at 287 nm, 327 nm and 400 nm.

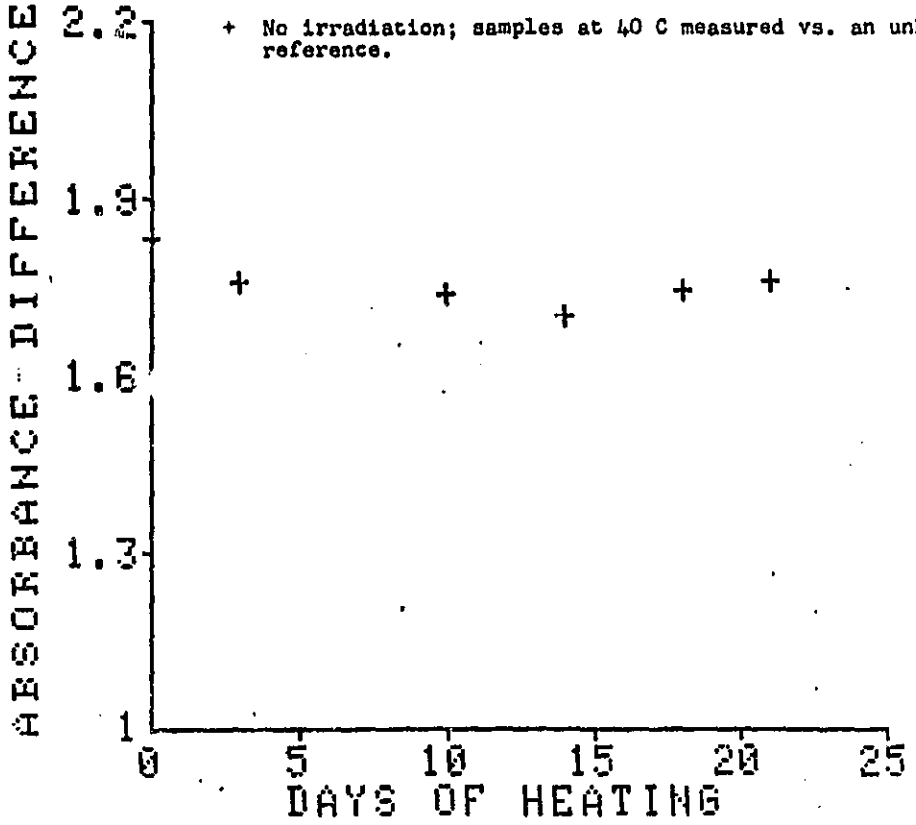

Fig. A2. A9918, crosslinked UV Abs. changes at 215 nm.